ON THE THEORY OF SALIENT POLE ALTERNATORS WITH ELECTROMAGNET AND WITH PERMANENT MAGNET EXCITATIONS

Thesis by

Peilin Luo

In Partial Fulfillment of the Requirements

For the Degree of

Doctor of Philosophy

California Institute of Technology

Pasadena, California

1952

ACKNOWLEDGMENT

The author wishes to express his deep gratitude to Dr. R. W. Sorensen for his constant encouragement and guidance, to the California Institute of Technology for granting a Francis J. Cole Scholarship which enabled this research program to be carried out, to the O'Keefe and Merritt Co. for providing a part of the fund necessary for the research and for supplying experimental data, and to Mr. C. J. Savant for valuable assistance.

ABSTRACTS

I THE SYNCHRONOUS REACTANCES OF ALTERNATORS WITH PERMANENT MAGNET EXCITATION AND ALTERNATORS WITH SKEWED ARMATURE SLOTS: The method for calculating the two reactances of salient pole alternators with permanent magnet excitation has been developed. Owing to the presence of the magnets, the direct axis armature reactance has been found to be much smaller than in electromagnet excited machines of similar sizes. The quadrature axis reactance is thus found to be likely the greater of the two.

The influence of skewing the armature slots has been studied, both for electromagnet excited and permanent magnet excited machines. It has been found that the general influence is to decrease the armature reaction reactances and to increase the leakage reactances. The influence upon the total reactances is to a certain extent to reduce the difference between the reactances along the two axes. Formulae are given for both types of excitation.

The practical correctness of the formulae when saturation is not appreciable has been confirmed indirectly by comparing calculated and tested regulation curves of two existing machines.

II THE CARDIOID DIAGRAM METHOD OF DETERMINING THE VOLTAGE REGULATION OF SALIENT POLE ALTERNATORS AND THE LOAD VOLTAGE INCREASE PHENOMENON IN ALTERNATORS WITH PERMANENT MAGNET EXCITATION: A graphical method has been developed for rapidly determining from two reactances the regulation of alternators for a wide range of power factor. The

same method is used to study the performance of alternators with permanent magnet excitation. The study shows that it is possible to develop a system applicable to uniform rising regulation curves over a wide range of power factors from unity to that due to purely inductive load.

III THE OPTIMUM PROPORTIONS OF THE FIELD STRUCTURE OF PERMANENT MAGNET EXCITED ALTERNATORS: The optimum design of the field structure of permanent magnet excited alternators with specified lengths of air gap and stability has been obtained for two types of problems; viz., 1) when given space, to find the required maximum flux density in the air gap, and 2) when both space and the air gap flux density are known and the requirement is minimum weight of the magnets. A method of specifying the stability of the excitation magnets has been suggested.

It has been shown that appreciable improvements are possible for many existing designs.

PART I

THE SYNCHRONOUS REACTANCES OF ALTERNATORS WITH PERMANENT MAGNET EXCITATION AND ALTERNATORS WITH SKEWED ARMATURE SLOTS

CONTENTS

I INTRODUCTION

II ARMATURE REACTION REACTANCES OF ALTERNATORS WITH PERMANENT MAGNET EXCITATION AND PARALLEL SLOTS: General Description of the Influence of the Presence of the Permanent Magnets - The Vital Problem - The Potential of The Pole Piece Produced by the Direct-Axis Reaction Field - The Calculation of A_{d1} - Formulae for the Direct- and the Quadrature-Axis Reaction Reactances.

III THE INFLUENCES OF SKEWING THE ARMATURE SLOTS AND THE SKEWING REACTANCES: Introduction - The Reactances arising from the Space Fundamental of the Reaction MMF - The Simplification to a Two-Dimensional Problem - The Intermingling Effect Between the Two Reactances - Case with E. M. Excitation - Case with P. M. Excitation - A Further Clarification of the Concept Pertaining to the Reaction Reactances - The Mutual Flux and the Reaction Reactances - The Skewing Reactances - Effect of Skewing upon the Slot and the Differential Leakage Reactances.

IV EXPERIMENTAL CONFIRMATION

V CONCLUSION

Appendix I: Flux Plotting in Presence of Permanent Magnets

Appendix II: Symbols and Definitions

References

PART II

THE CARDIOID DIAGRAM METHOD OF DETERMINING THE VOLTAGE REGULATION OF SALIENT POLE ALTERNATORS AND

THE LOAD VOLTAGE EXALTATION PHENOMENON IN ALTERNATORS WITH PERMANENT MAGNET EXCITATION

I THE CARDIOID DIAGRAM

II THE UNIVERSAL CARDIOID GRAPH PAPER

III AN EXAMPLE OF THE USE OF THE CARDIOID GRAPH PAPER

IV THE LOAD VOLTAGE EXALTATION PHENOMENON IN THE ALTERNATORS WITH PERMANENT MAGNET EXCITATION

V CONCLUSION

PART III

THE OPTIMUM PROPORTIONS OF THE FIELD STRUCTURE OF PERMANENT MAGNET EXCITED ALTERNATORS

I GENERAL: Introduction - Specification of the Stability - Estimation of - The Length of the Air Gap - Simplification of the Problem.

II THE OPTIMUM PROPORTION FOR A MAXIMUM AIR GAP FLUX DENSITY: The Magnetic Constraint - The Dimensional Constraint - Stabilization on the Lower Part of the Demagnetization Curve - Stabilization on the Upper Part of the Demagnetization Curve - Stabilization at the Knee.

III THE OPTIMUM PROPORTION FOR A MINIMUM WEIGHT OF MAGNETS WITH SPECIFIED AIR GAP FLUX DENSITY: The Constraint of the Problem - Stabilization on the Lower Part of the Demagnetization Curve - Stabilization on the Upper Part of the Demagnetization Curve - Stabilization at the Knee.

IV CONCLUSION AND DISCUSSION

Appendix I: Derivation of Formula 1

Appendix II: Derivation of Formulae 3 and 19

Appendix III: Derivation of other Formulae

Appendix IV: List of Symbols

References

PART I

THE SYNCHRONOUS REACTANCES OF ALTERNATORS

THE SYNCHRONOUS REACTANCES OF ALTERNATORS WITH PERMANENT MAGNET EXCITATION AND ALTERNATORS WITH SKEWED ARMATURE SLOTS

I INTRODUCTION

The prediction of the regulation of the electromagnet excited alternators by means of calculations based upon the two reactances χ_q and χ_d has been a well established technique since the early thirties. Very elaborate formulae for the calculation of these reactances have been sufficiently developed to yield satisfactory accuracy for such type of alternators. Nevertheless, there is enough difference between the construction of the electromagnet excited machines and the permanent magnet excited machines to invalidate for the latter case the use of the standard reactance formulae. Also, there are not yet available satisfactory formulae for the reactances when the armature slots are skewed. The purpose of this paper is thus to present the development of reactance formulae when these factors are present.

The author does not intend to make this paper a complete account of all phases of alternator reactances. Interested readers are referred to any standard textbook on alternating current machines.* However, when the armature slots are skewed, the reactance definitions need additional clarification as will be discussed in the third section of this paper. Moreover, it is found helpful to unify the definitions used in this thesis. Therefore, a concise table classifying the reactances according to (1) the part of the conductors linking the part or component of the flux associated with a specific reactance, (2) the location of the part

* For a general knowledge of the several reactances of e.m. excited machines, the readers are referred to Reference 4 at the end of this paper.

or component of the flux, and (3) the space frequency order of the m.m.f. distribution producing the part or component of the flux, is included herewith.

Only the unsaturated reactances will be considered in this paper.

II ARMATURE REACTION REACTANCES OF ALTERNATORS WITH P. M. EXCITATION AND PARALLEL SLOTS

GENERAL DESCRIPTION OF THE INFLUENCE OF THE PRESENCE OF THE MAGNETS: The point most relevant to the entire theory of unsaturated reactances is the hypothetical linearity of the magnetic circuit. Moreover, in the case of the electromagnet excited machines, the ferromagnetic part of the magnetic circuit is assumed to possess an infinite permeability. The justification for these assumptions depends upon the actual working point of the magnetization curve and the properties of the magnetic materials used in the magnetic circuit. The accuracy of result, based upon the foregoing assumptions, should always be carefully scrutinized. Fortunately, the situation is much better in the case of p.m. machines. All commonly encountered p. m. materials possess rather low values of incremental permeability of almost constant magnitude within the ordinary range of operation. Along the direct axis, the magnet and the air gap contribute the major part of the reluctance even at the higher ranges of flux density. Consequently, the direct axis reactance is very low and almost constant. Because of this advantage, the use of unsaturated reactances in calculations for the prediction of the regulation for p.m. machines appears to give results much more accurate and, hence, more valuable than in the e.m. case, even though the scant data available with p.m. machines at present are not yet sufficient for the full development of empirical rules for calculating the saturated values.

Along the quadrature axis of armature reaction, the part of the magnetic circuit lying in the rotor consists, in general, of two parallel branches formed by the permanent magnet and the pole piece. Since the pole piece possesses relatively high permeance, the quadrature flux is very little affected by the presence of the permanent magnet. Consequently, if the length of the air gap remained the same, the quadrature axis reactance would be almost unaffected by the insertion of the permanent magnet.

The most striking influence of the presence of the permanent magnet becomes obvious. In contrast with the e.m. case, the quadrature axis reaction reactance of a p.m. alternator is the greater of the two, even though it may be smaller in magnitude than that for a similar machine with e.m. excitation when the field is saturated. The relatively lower direct axis reactance gives rise to a much better regulation with inductive load for p.m. than for e.m. machines. The strange combination of a small direct axis reactance with a greater quadrature axis reactance is responsible for a comparatively small voltage regulation, sometimes even a rising one, at unity power factor. These facts make possible the use in p.m. machines of a smaller air gap than would be suitable for e.m. machines of like rating. This effect, owing to the effect of the permanent magnet, increases both reactances, the increase in the quadrature axis being greater than the increase in the direct axis reactance. This situation further magnifies the differences between the characteristics of the e.m. machine and that of the p.m. machine.

THE KERNEL PROBLEM: The complications arising from the presence

SUB-COMPONENTS OF DIRECT-AXIS AND QUADRATURE-AXIS SYNCHRONOUS REACTANCES

<table>
<tr><td rowspan="5">Linkage with embedded part of conductor</td><td rowspan="3">Flux in region external to armature surface

Air gap reactance</td><td rowspan="2">Flux due to axial component of current distribution</td><td colspan="3">Flux penetrating into field structure

Armature reaction reactance</td></tr>
<tr><td>Flux due to space harmonics of current distribution

Differential reactance</td><td>Pole frequency

Belt Leakage reactance</td><td rowspan="3">Flux not penetrating into the field structure

Leakage reactance</td></tr>
<tr><td colspan="2">Flux due to peripheral component of current distribution

Skewing reactance</td><td>Tooth frequency zigzag and tooth-tip reactance</td></tr>
<tr><td colspan="4">Flux in slots

Slot reactance</td></tr>
<tr><td colspan="4">Linkage with end connections

End connection reactance</td></tr>
</table>

of the permanent magnets have been reduced to a special procedure for the calculation of the factor A_{d1} by standard formula. However, due to the peculiar configurations of the pole pieces encountered in the p. m. alternators and the meagerness of data obtained from tests on existing designs, empirical rules, comparable in simplicity with those for e.m. machines, are still unavailable. A general method applicable to a very wide variety of pole pieces is presented.

THE POTENTIAL OF THE POLE PIECE UNDER THE ACTION OF THE DIRECT AXIS REACTION FIELD: With the direct axis reaction m.m.f. acting alone, with no magnetization in the magnet, since the magnet offers a large reluctance, the pole piece would assume a potential ψ_p other than zero.

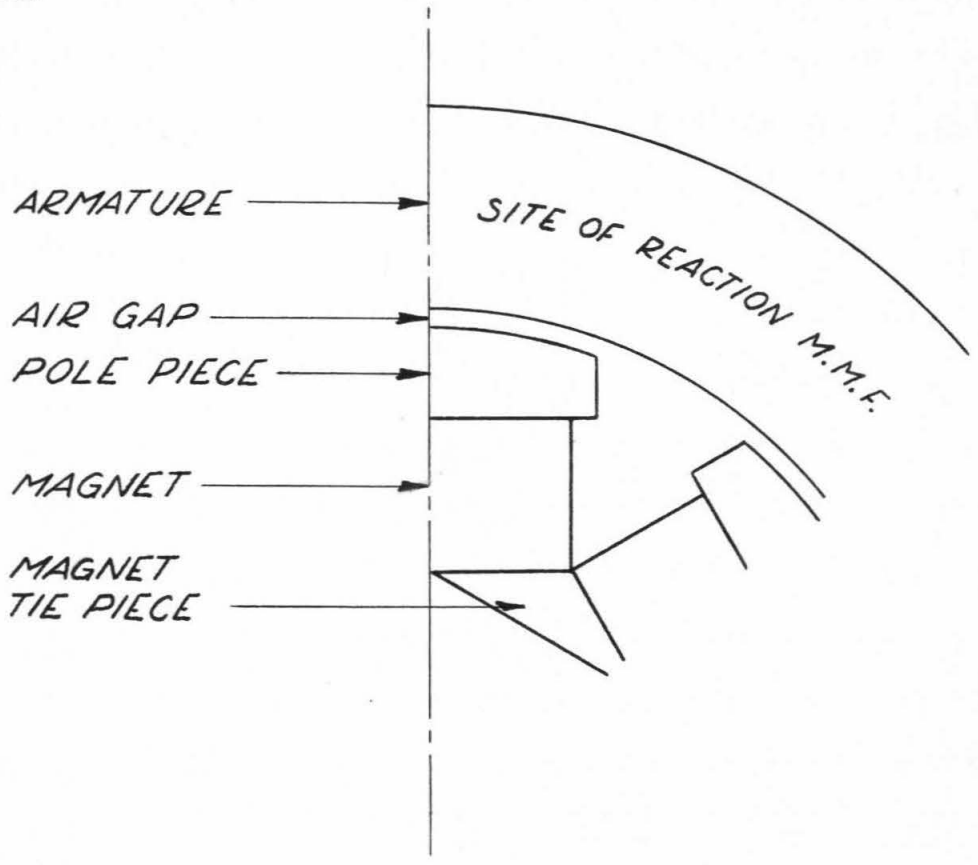

Fig. 1

The determination of the potential ψ_p is based upon the principles of replacement and superposition. First, a flux plot* is made as though direct axis armature reaction only were present with the pole piece at zero potential. In other words, the magnet is assumed to have zero reluctance. An example of this "direct axis reaction flux plot" is shown in Fig. 2. From this plot, the ratio of the number of squares along the whole periphery of the pole piece, N_{tfd}, to the number of squares along a tube of force between the pole face and the armature surface at the center of the pole, N_{psd}, is computed.

A flux plot is then made by assuming the pole piece to be at an arbitrary potential and the armature surface at zero potential. The permeability of the magnet is assumed to be μ_Δ in this case. An example is shown in Fig. 3. From this plot, the ratio of the number of squares along the whole periphery of the pole piece, N_{tfe}, to the number of squares along a tube of force, N_{pse}, is computed.

Then,

$$\psi_p / \hat{F} = (N_{tfd}/N_{psd}) / (N_{tfe}/N_{pse}) \qquad (1)$$

where $\hat{F}$ is the maximum value of the space fundamental of the armature reaction m.m.f. due to the fundamental current.

CALCULATION OF A_{d1} : The value of A_{d1}, defined as the ratio of the amplitude of the fundamental component of the flux wave produced by the direct axis m.m.f. alone, to the maximum value of what the flux density would be if the air gap was uniform everywhere (i.e., for a hypothetical non-salient pole machine with same length of air gap as the one at the

---

* For the method of flux plotting in the presence of permanent magnets, see Appendix I.

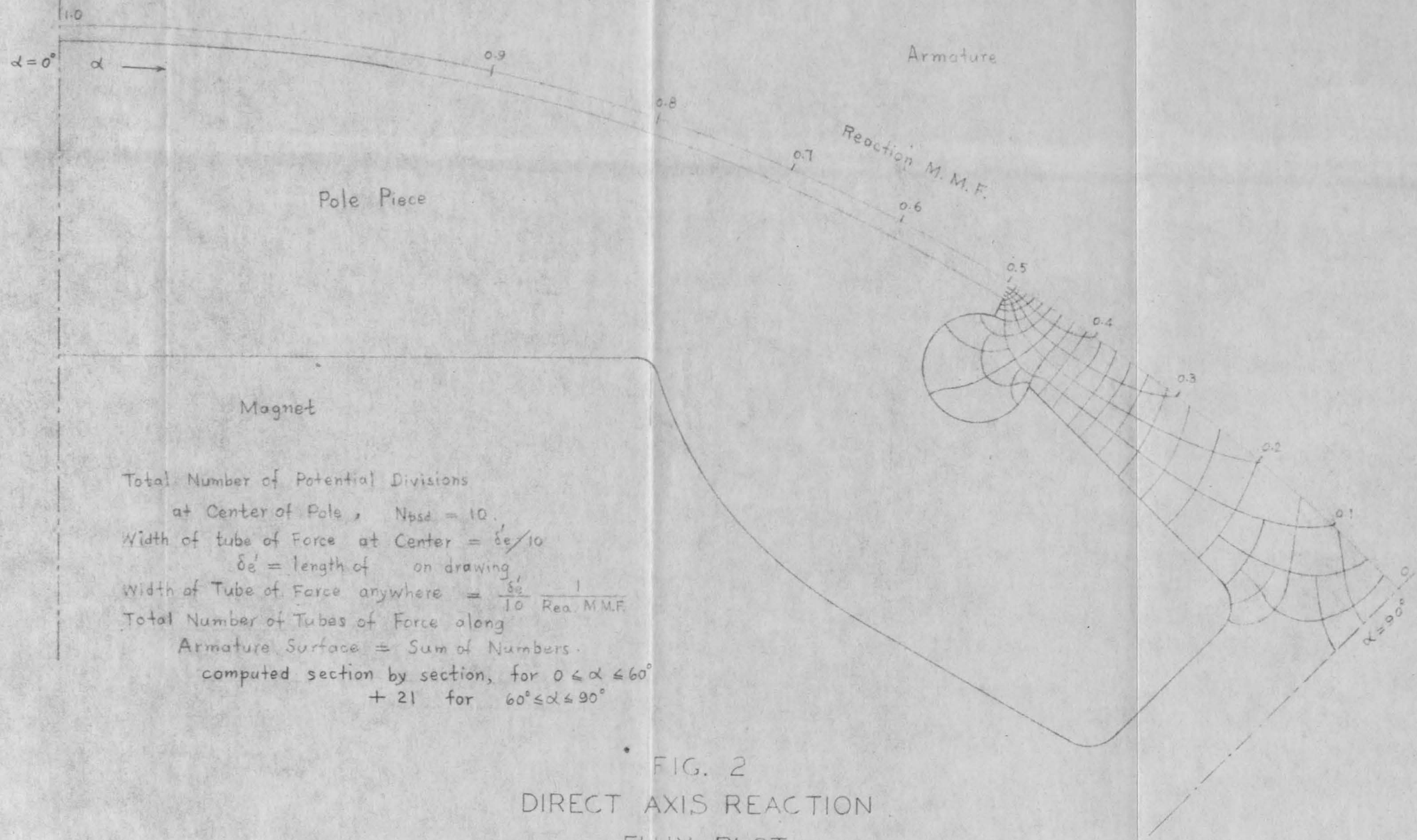

Total Number of Potential Divisions
at Center of Pole, $N_{psd} = 10$.
Width of tube of Force at Center $= \delta e'/10$
$\delta e'$ = length of on drawing
Width of Tube of Force anywhere $= \frac{\delta e'}{10} \frac{1}{\text{Rea. M.M.F.}}$
Total Number of Tubes of Force along
Armature Surface = Sum of Numbers
computed section by section, for $0 \leq \alpha \leq 60°$
$+ 21$ for $60° \leq \alpha \leq 90°$

FIG. 2
DIRECT AXIS REACTION
FLUX PLOT

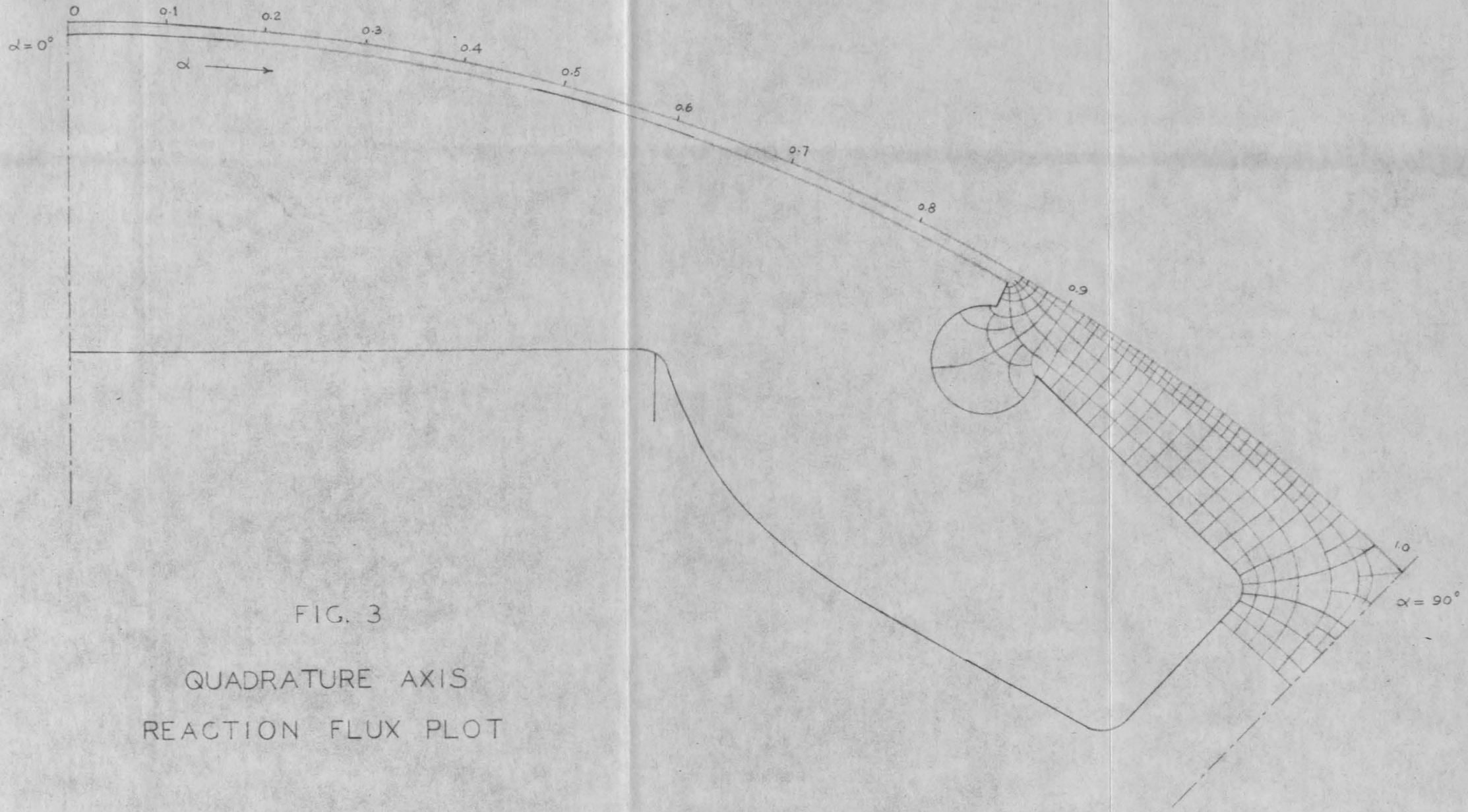

FIG. 3

QUADRATURE AXIS

REACTION FLUX PLOT

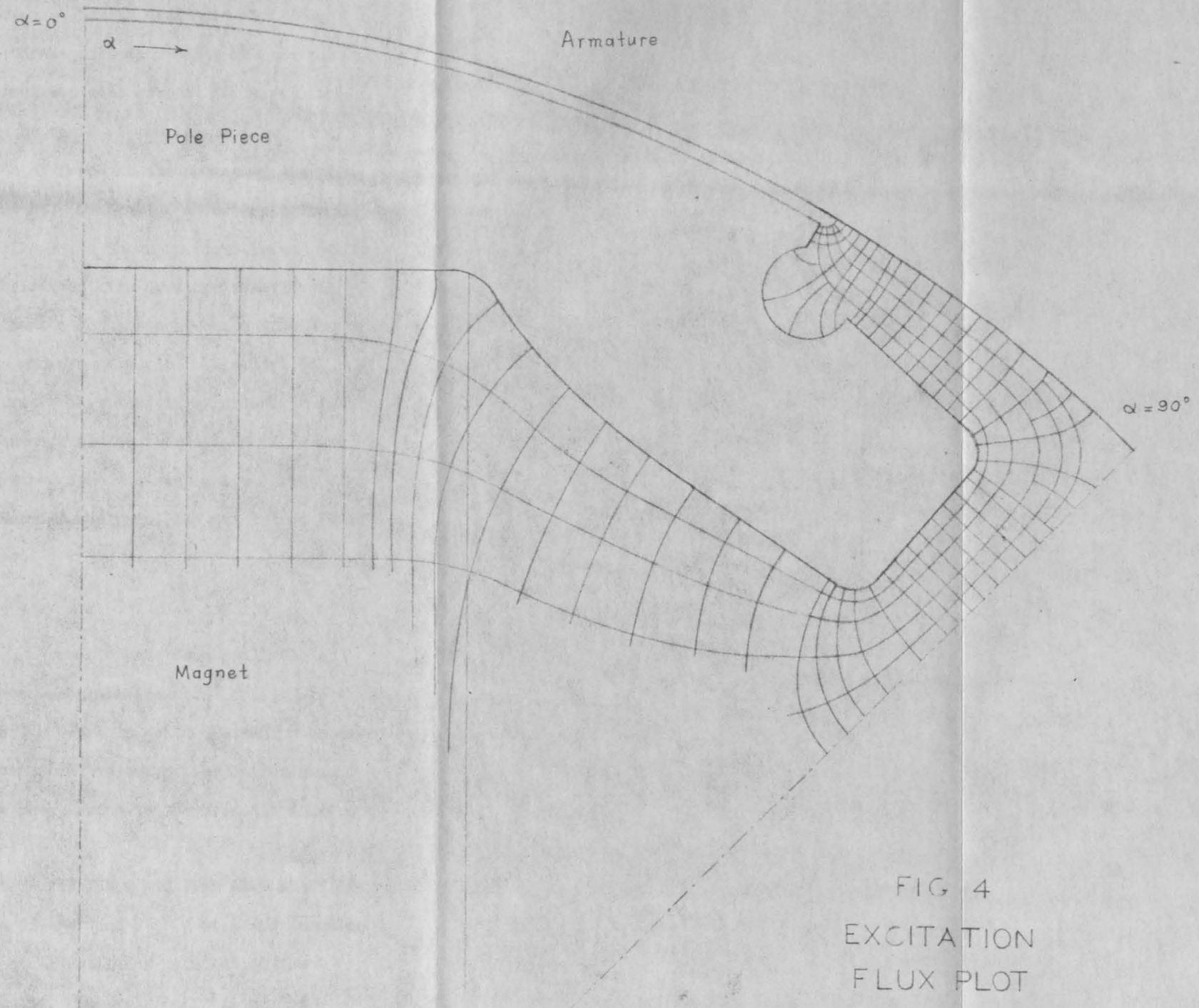

FIG 4
EXCITATION
FLUX PLOT

center of the pole in the actual case). This is again determined by a method of superposition. From the direct axis flux plot, the corresponding air gap flux density curve, normalized with respect to its maximum value, may be obtained by plotting the ratio of the length along the armature surface subtended by a tube of force at the center of the pole, to the same quantity at the field point. Similarly, a curve can be plotted for the excitation flux plot. These are shown in Figs. 5a and 5b. The total flux density curve for the direct axis armature reaction is readily obtained by adding to the first one the second one multiplied by the value of $\psi_p/\hat{F}$ given by (1) as shown in Fig. 5c. Actually, it is not necessary to plot this third curve. The respective ratios, A'_{d1} and A_{e1}, of the amplitudes of the fundamentals to the maximum values at the center of the pole can be determined from the respective curves Fig. 5a and Fig. 5b by straightforward Fourier analysis. By the principle of superposition, the value of A_{d1} is:

$$A_{d1} = A'_{d1} - (\psi_p/\hat{F})\, A_{e1} \qquad (2)$$

In actual design work, $A_{e1} = f_b f_d$ should have been available at this stage, so it is not necessary to calculate again.

It must be observed that, although A'_{d1} is defined exactly the same as the A_{d1} in e.m. case, the conventional values of the latter should not be used for A'_{d1} in the present case, owing to the mardedly different shapes of the poles.

THE FORMULAE FOR THE DIRECT AXIS- AND THE QUADRATURE AXIS-REACTION REACTANCES: With the proper values of A_{d1} and A_{q1}, standard formulae for the e.m. machines may be used equally well for calculating the reaction reactances of the p.m. machine. The value of A_{q1} may be

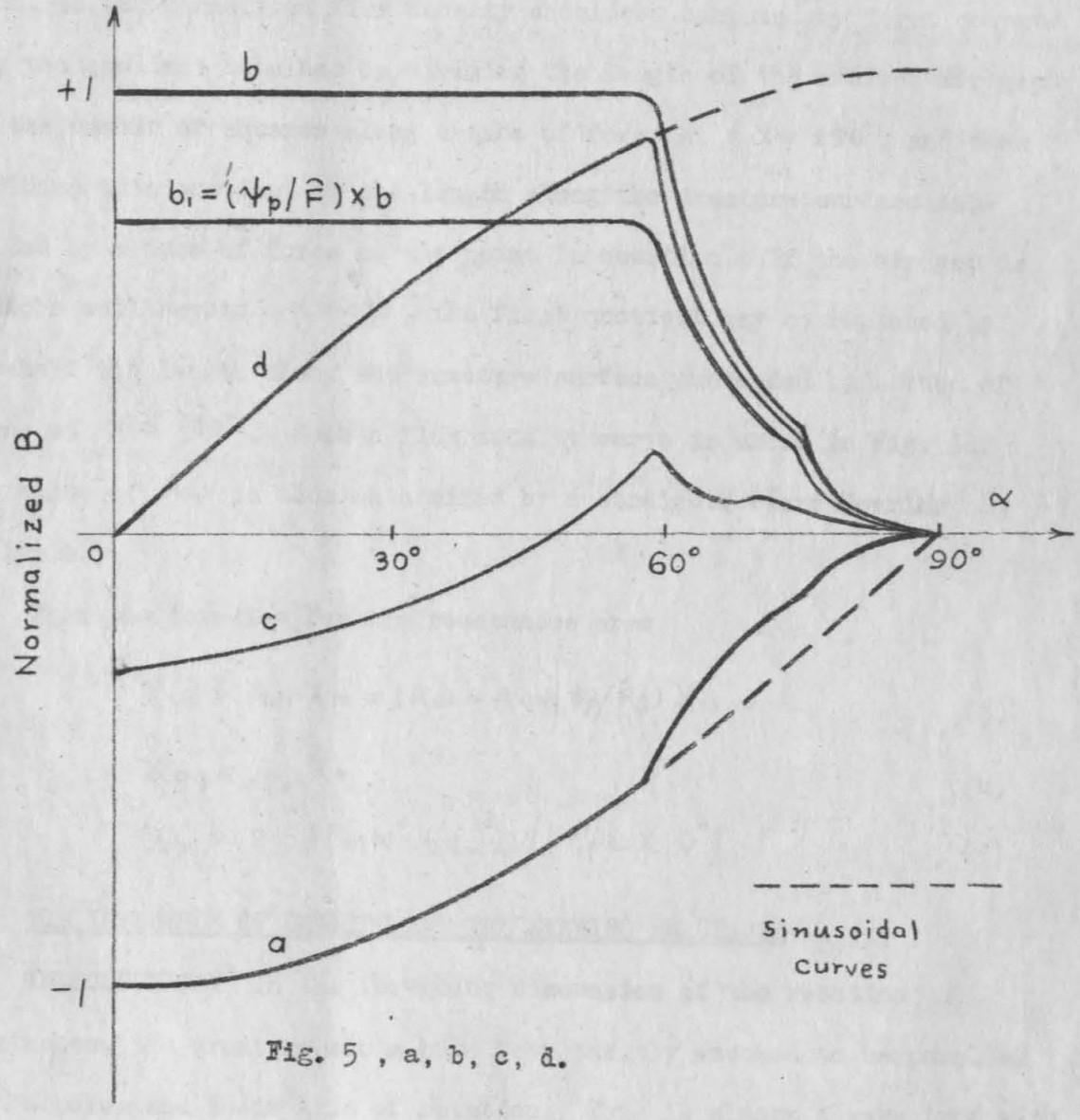
+1
b
$b_1 = (\psi_p / \hat{F}) \times b$
d
Normalized B
0
30°
60°
90°
α
c
a
-1
Sinusoidal
Curves

Fig. 5 , a, b, c, d.

determined from a quadrature axis flux plot as shown in Fig. 4 in a manner similar to that just described for finding A_{d1}. In this case, the normalized flux density for the hypothetical non-salient pole case is to be taken at $\alpha = \pm 90^\circ$ and cannot be obtained directly from the plot, so the normalized flux density should be computed by first computing the quotient obtained by dividing the length of the minimum air gap by the number of squares along a tube of force at $\alpha = \pm 90^\circ$, and then dividing this quotient by the length along the armature surface subtended by a tube of force at the point in question. If the air gap is uniform well beyond $\alpha = \pm 30^\circ$, the first quotient may be replaced by one-half the length along the armature surface subtended by a tube of force at $\alpha = \pm 30^\circ$. Such a flux density curve is shown in Fig. 5d. The value of A_{q1} is then determined by a straightforward Fourier analysis.

Then the formulae for the reactances are:

$$\chi_{ad} = A_{d1}\chi_m = (A'_{d1} - A_{e1}\{\psi_p/\hat{F}\})\chi_m \qquad (3)$$

$$\chi_{aq} = A_{q1}\chi_m \qquad (4)$$

$$\chi_m = 2{\cdot}5 f l_m N^2 (f_c f_w)^2 D / (n_p^2 \delta_e \times 10^6) \qquad (5)$$

III THE INFLUENCE OF SKEWING AND THE SKEWING REACTANCE

INTRODUCTION: In the foregoing discussion of the reaction reactances, the armature slots have been tacitly assumed to be parallel to the poles and their axis of rotation. This is almost always true with the e.m. machines which have chamfered pole pieces to produce tapering of the air gap at the pole tips. The latter fact explains the scarcity of current literature pertaining to the influences of skewing the slots.

Since skewing is very often used in the p.m. machines, special formulae will be derived to take this into account.

THE REACTANCES ARISING FROM THE SPACE FUNDAMENTAL OF THE REACTION MAGNETOMOTIVE FORCE: In the theory regarding the unskewed case, the reactances associated with the space fundamental of the reaction magnetomotive forces are identified with the armature reaction. When the skewing is appreciable, however, this is no longer true as will be seen in a later section. The general tendency of skewing is to decrease the armature reaction and to increase the leakage; the latter being subject to analysis as an additional term identified as the skewing reactance and having in general different values in the direct and the quadrature axes. In what follows, the reactances arising from the space fundamental will first be treated as an integral term.

THE SIMPLIFICATION TO A TWO-DIMENSIONAL PROBLEM: In the unskewed case, the simplification of the problem to a two-dimensional one has been justified on the hypothetical condition that the end effect upon the armature reaction is negligible and may be corrected subsequently by using an adjusted length of armature in the calculation. When the skewing is appreciable, this alone will not suffice. Since the equi-reaction mmf contours on the armature surface are skewed with respect to the axis, there will be flux component in the longitudinal direction. In the presence of such flux, the two-dimensional counter part is even a poorer approximation. Fortunately, most of the flux concentrates either in, or in the vicinity of the air gap. In this region, because of the high permeability of the iron parts, the flux is almost perpendicular to the iron surfaces and, hence, has a small longitudinal component. The rest of the flux, not being in

the air gap region, contributes little to the reaction voltage and the correction required for it is of a low order of magnitude. Owing to that fact, the simplification to a two-dimensional problem is practically justified for an infinitesimal slice of the air space. Thus, all expedients such as the flux plots and the Fourier coefficients A_{d1} and A_{e1}, which have been employed in the foregoing analysis are available for use in the present work.

THE INTERMINGLING EFFECT BETWEEN THE DIRECT AXIS AND THE QUADRATURE AXIS REACTANCE TERMS: Because of the type of symmetry prevailing in a skewed conductor, the resultant e.m.f. induced in the latter is in phase with that induced in an infinitesimal length at the center only. The e.m.f. induced in any other infinitesimal length is progressively different in phase. Thus, the direct axis component of the load current, originally being identified with respect to the resultant e.m.f. must have a quadrature component when it is referred to any infinitesimal e.m.f. other than that at the center. The reverse is true with the quadrature axis component. Consequently, the expression for the voltage drop produced by either the direct axis or the quadrature axis current consists of terms containing both the unskewed direct axis and the unskewed quadrature axis reactances. As will be shown in the forthcoming analyses, the skewed values of the reactances are linear combinations of the two unskewed values. When the skewing is impractically excessive, the tendency is to level out the difference between the two skewed values and ultimately bring them to the same average between the two unskewed values with zero magnet reluctance.

CASE WITH E.M. MACHINE, i.e., WITH ZERO MAGNET RELUCTANCE: The

e.m.f. induced in an infinitesimal length of conductor is $e^{-j\theta}(E'd\xi/l)$ where E' is the open circuit induced e.m.f. in the whole conductor if the skewing were absent, ξ is the coordinate representing the longitudinal position, l is the length of the armature, and θ is defined by $\theta_{sk}\xi/l$, hence $d\xi/l = d\theta/\theta_{sk}$

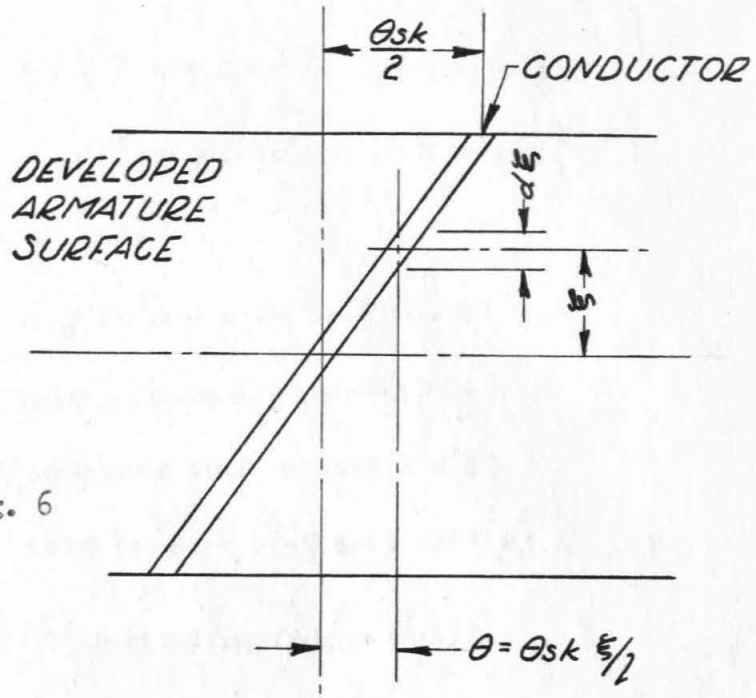

Fig. 6

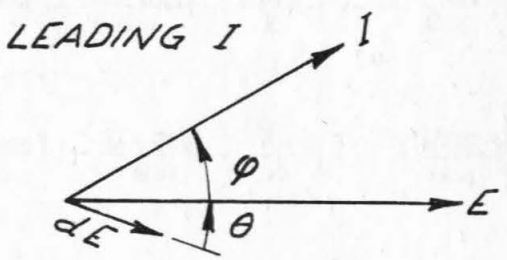

Fig. 7

θ_{sk} being the angle of skewing in electrical radians. With the simplification to two dimensions, this infinitesimal length of the armature may be treated as an individual generator with reaction reactances $\chi'_{ad}\,d\xi/l$ and $\chi'_{aq}\,d\xi/l$ where the prime indicates an unskewed value with zero magnet reluctance, the configuration in the air gap remaining the same. The load current consists of the direct component $I\sin\varphi$ and the quadrature component $I\cos\varphi$, both referred to the resultant e.m.f. With the resistance neglected for the present, the voltage relation holding for the infinitesimal generator is thus

$$dE = \frac{d\xi}{l} e^{j\theta} \Big\{ E' - \chi'_{ad} (I \sin\varphi \cos\theta - I \cos\varphi \sin\theta) - j \chi'_{aq} (I \cos\varphi \cos\theta - I \sin\varphi \sin\theta) \Big\}$$

$$= \frac{d\theta}{\theta_{sk}} \Big\{ E' (\cos\theta - j \sin\theta) + I \chi'_{ad} (\sin\varphi \cos^2\theta + \cos\varphi \sin\theta \cos\theta) - I \chi'_{aq} (\cos\varphi \sin\theta \cos\theta + \sin\varphi \sin^2\theta) - j I \chi'_{ad} (\sin\varphi \cos\theta \sin\theta + \cos\varphi \sin^2\theta) - j I \chi'_{aq} (\cos\varphi \cos^2\theta + \sin\varphi \sin\theta \cos\theta) \Big\} \quad (6)$$

The resultant voltage is obtained by integrating from $-\theta_{sk}/2$ to $\theta_{sk}/2$, #

$$E = E' \frac{\sin(\theta_{sk}/2)}{\theta_{sk}/2} - I \sin\varphi \left\{ \frac{\chi'_{ad}}{2} \left(1 - \frac{\sin\theta_{sk}}{\theta_{sk}} \right) - \frac{\chi'_{aq}}{2} \left(1 - \frac{\sin\theta_{sk}}{\theta_{sk}} \right) \right\}$$

$$- j I \cos\varphi \left\{ \frac{\chi'_{aq}}{2} \left(1 - \frac{\sin\theta_{sk}}{\theta_{sk}} \right) - \frac{\chi'_{ad}}{2} \left(1 - \frac{\sin\theta_{sk}}{\theta_{sk}} \right) \right\} \quad (7)$$

Thus, two reactances arising from the space fundamental of the armature reaction m.m.f. may now be defined:*

$$\chi_{d1} = \frac{\chi'_{ad}}{2} \left(1 - \frac{\sin\theta_{sk}}{\theta_{sk}} \right) - \frac{\chi'_{aq}}{2} \left(1 - \frac{\sin\theta_{sk}}{\theta_{sk}} \right) \quad (8)$$

$$\chi_{q1} = \frac{\chi'_{aq}}{2} \left(1 - \frac{\sin\theta_{sk}}{\theta_{sk}} \right) - \frac{\chi'_{ad}}{2} \left(1 - \frac{\sin\theta_{sk}}{\theta_{sk}} \right) \quad (9)$$

At the sacrifice of some clearness in physical interpretation, the same may be derived with greater mathematical elegance as follows:

$$dE = \left\{ E' + I \chi'_{ad} \sin(\theta+\varphi) - j I \chi'_{aq} \cos(\theta+\varphi) \right\} e^{j\theta} d\xi / l = \left\{ E' e^{j\theta} - \tfrac{1}{2} j I \chi'_{ad} \left[e^{j\varphi} - e^{-j(\varphi+2\theta)} \right] - \tfrac{1}{2} j I \chi'_{aq} \left[e^{j\varphi} + e^{-j(\varphi+2\theta)} \right] \right\} \frac{d\theta}{\theta_{sk}} \quad (11)$$

$$E = E' (\sin \tfrac{\theta_{sk}}{2} / \tfrac{\theta_{sk}}{2}) - j \frac{\chi'_{ad}}{2} \left[e^{j\varphi} - e^{-j\varphi} \left(\frac{\sin\theta_{sk}}{\theta_{sk}} \right) \right] - j \frac{\chi'_{aq}}{2} \left[e^{j\varphi} + e^{-j\varphi} (\sin\theta_{sk} / \theta_{sk}) \right] \quad (12)$$

* For non-salient pole construction, $\chi'_{ad} = \chi'_{aq} = \chi_a$, $\chi_a = \chi_q = \chi_a$ which conforms with the statement of Morril.

and the open circuit e.m.f. is:*

$$E = E'' \frac{\sin(\theta_{sk}/2)}{\theta_{sk}/2} \qquad (10)$$

As a consequence of these expressions, the two reactances tend to the same value $\frac{1}{2}(\chi'_{ad} + \chi'_{aq})$ as θ_{sk} increases indefinitely.

CASE WITH PERMANENT MAGNET GENERATOR, I.E., NON-ZERO MAGNET RELUCTANCE: The Reactional Magnetic Potential of the Pole Piece. Being similar to the case without skewing present, the determination of the reactances in the presence of the magnet, again hinges around the magnetic potential of the pole piece under the action of the reaction m.m.f. On account of the presence of this potential, the analysis for this case must be carried back to the distribution of the reaction magnetomotive force, instead of starting from the unskewed reactances, as in the case of zero magnet reluctance. The reaction magnetomotive force as a function of both the longitudinal and the peripherial positions is resolved into four components each being distributed with a different combination of types of symmetry with respect to the longitudinal and the peripherical coordinates. Two of these components produce a direct axis reaction and the remaining two a quadrature axis reaction. Again two reactances are defined. It is found that only the component which is symmetrical with respect to both coordinates yields a flux passing through the magnet, so the consideration of the potential mentioned above is involved in this component only.

---

* Bewley derived the same expression for the open circuit voltage but did not carry out the analysis of the reaction.

THE FOUR COMPONENTS: With skewing present, the magnetomotive force at any point on the armature surface, specified by the longitudinal coordinate ξ in linear measure and the peripherial coordinate α in electrical angular measure, is given by:

$$F = \hat{F} \sin(\alpha - \xi \theta_{sk}/l - \varphi), \tag{13}$$

where the center of the pole face is taken as the origin and φ is the phase angle of the load current with respect to the open circuit voltage.

This expression is readily expanded to:

$$F = -\hat{F} \sin\varphi \cos(\alpha - \xi \theta_{sk}/l) + \hat{F} \cos\varphi \sin(\alpha - \xi \theta_{sk}/l), \tag{14}$$

in which, if θ_{sk} is zero, the two right-hand terms are readily identified as the direct axis and the quadrature axis reactions respectively.

Further expansion of the expression yields:

$$\begin{aligned} F &= -\hat{F} \sin\varphi \cos\theta \cos\alpha - \hat{F} \sin\varphi \sin\theta \sin\alpha + \hat{F} \cos\varphi \cos\theta \sin\alpha - \hat{F} \cos\varphi \sin\theta \cos\alpha \\ &= -F_{de} - F_{do} + F_{qe} - F_{qo}, \end{aligned} \tag{15}$$

in which the subscripts have the following significances:

d - arising from direct axis current,

q - arising from quadrature axis current,

e - even symmetry in longitudinal direction, and

o - odd symmetry in logitudinal direction.

The different types of symmetry for the four components are shown in Figs. 8 and 9.

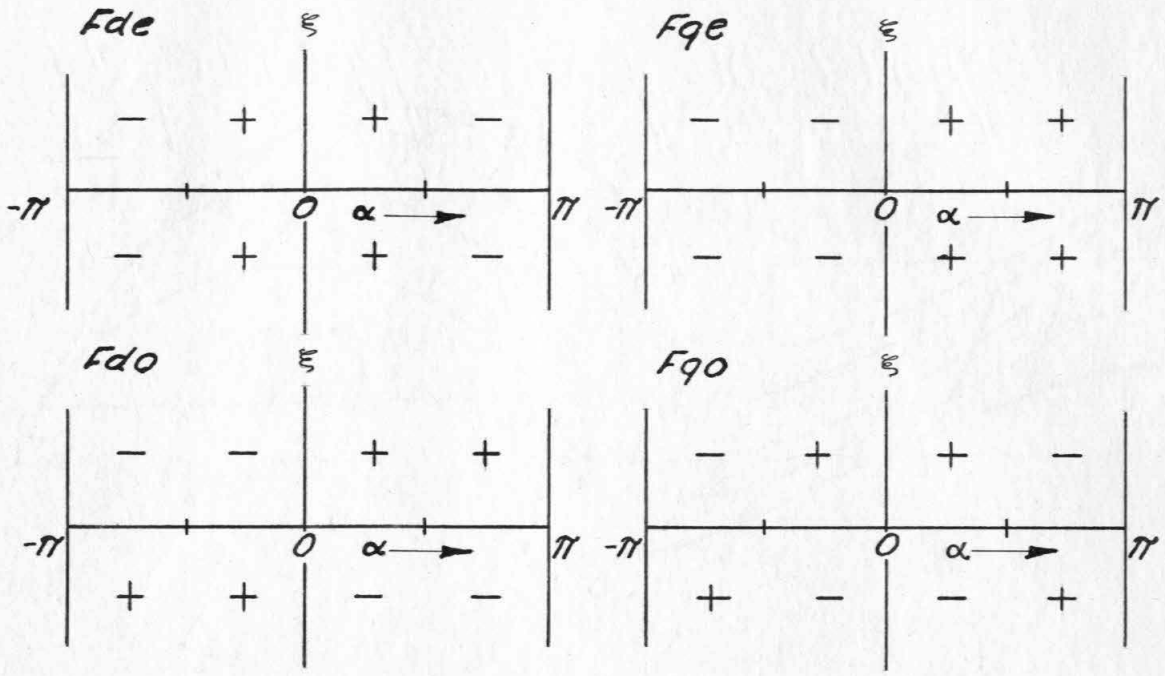

Fig. 8

Symmetry in M.M.F. Distribution

THE DIRECT AXIS COMPONENT WITH EVEN SYMMETRY: This component has even symmetry with respect to both α and θ, $(=\theta_{sk}\xi/l)$. Thus, it yields a finite, nonvanishing net flux through the magnet unless $\theta_{sk} =$ a multiple of $2\pi, \neq 0$, which is unlikely to occur. The net flux passing through the magnet is evaluated in a manner quite similar to that in the case without skewing. In the present case, a slice of the pole piece of thickness $d\xi$, is first considered. The flux entering this slice is:

$$\left(\frac{N_{tfd}}{N_{psd}} \hat{F} \sin\varphi \cos\frac{\theta_{sk}\xi}{l} - \frac{N_{tfe}}{N_{pse}} \psi_p \right) d\xi \quad , \tag{16}$$

where the N's have the same significance as in equation (3). The integral of this expression from $-l/2$ to $+l/2$ gives the total flux entering the pole piece, which must be zero:

$$l \left(\frac{N_{tfd}}{N_{psd}} \hat{F} \sin\varphi \cdot \frac{2}{\theta_{sk}} \sin(\theta_{sk}/2) - \frac{N_{tfe}}{N_{pse}} \psi_p \right) = 0 \quad , \tag{17}$$

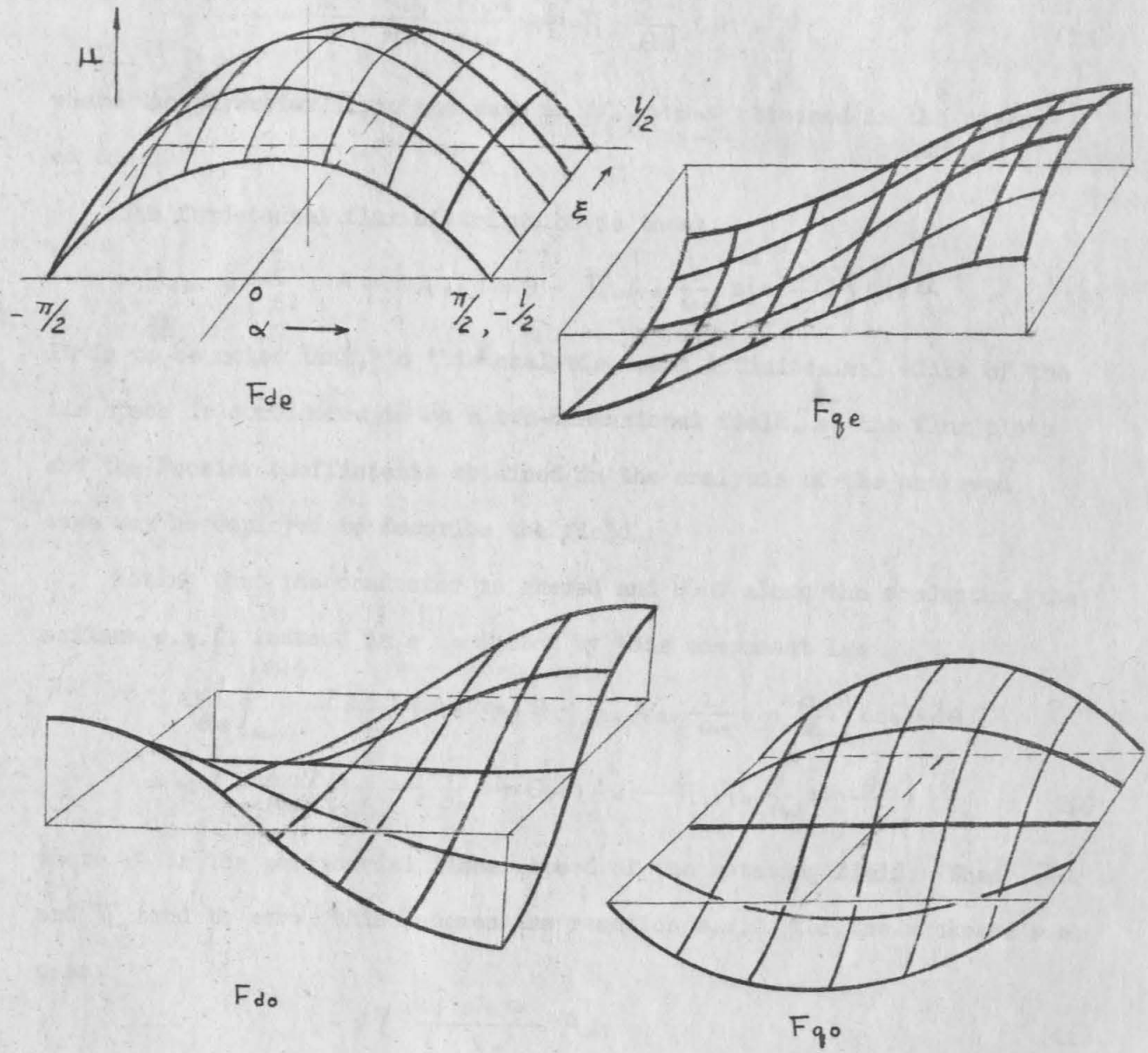

Reliefs Showing the Four
Components of F

Fig. 9

From this, we obtain:

$$\frac{\psi_p}{\hat{F}\sin\varphi} = \frac{2}{\theta_{sk}} \frac{N_{tfd}}{N_{tfe}} \frac{N_{pse}}{N_{psd}} \sin\frac{\theta_{sk}}{2} = \Pi_o \frac{2}{\theta_{sk}} \sin\frac{\theta_{sk}}{2} \tag{18}$$

where the parameter Π_o is the same as $\psi_p / \hat{M}\sin\varphi$ obtained in the unskewed case.

The fundamental flux distribution is then:

$$B_{de1} = -\frac{\hat{F}}{\delta_e} \sin\varphi \left\{ A'_{d1} \cos\theta - \Pi_o A_{e1} \frac{2}{\theta_{sk}} \sin\frac{\theta_{sk}}{2} \right\} \cos\alpha \tag{19}$$

It is to be noted that, in this analysis, each infinitesimal slice of the air space is considered to be a two-dimensional field, so the flux plots and the Fourier coefficients obtained in the analysis of the unskewed case may be employed to describe the field.

Noting that the conductor is skewed and $\alpha = \theta$ along the conductor, the maximum e.m.f. induced in a conductor by this component is:

$$-\frac{v l}{\theta_{sk}} \int_{-\theta_{sk}/2}^{\theta_{sk}/2} \frac{\hat{F}\sin\varphi}{\delta_e} \left\{ A'_{d1} \cos\theta - \Pi_o A_{e1} \frac{2}{\theta_{sk}} \sin\frac{\theta_{sk}}{2} \right\} \cos\theta \, d\theta$$

$$= -v l \frac{\hat{F}\sin\varphi}{\delta_e} \left\{ \left(\frac{1}{2} + \frac{1}{2}\frac{1}{\theta_{sk}} \sin\theta_{sk}\right) A'_{d1} - \Pi_o A_{e1} \frac{2}{\theta_{sk}} \sin\frac{\theta_{sk}}{2} \right\} \tag{20}$$

where v is the peripherial linear speed of the rotating field. When θ_{sk} and Π_o tend to zero, this becomes the reaction e.m.f. for the unskewed e.m. case:

$$-v l \frac{\hat{F}\sin\varphi}{\delta_e} A'_{d1} \tag{21}$$

The ratio of the two e.m.f.'s is equal to the ratio of the two reactances in the two cases, hence a component reactance may be defined for the present case:

$$\chi_{ade} = \chi'_{ad} \left\{ \left(\frac{1}{2} + \frac{1}{2}\frac{\sin\theta_{sk}}{\theta_{sk}}\right) - \Pi_o \frac{A_{e1}}{A'_{d1}} \frac{\sin(\theta_{sk}/2)}{\theta_{sk}/2} \right\} \tag{22}$$

which is a part of the direct axis reactance.

THE DIRECT AXIS COMPONENT WITH ODD SYMMETRY: Since the distribution of the m.m.f. and hence that of the flux is anti-symmetrical with respect to ξ , it yields no flux passing through the magnet. Since the flux distribution is also anti-symmetrical with respect to α , the reaction e.m.f. is a maximum when the center point of the conductor coincides with the origin; hence it is a direct axis component.

The fundamental component of the flux is readily found to be:

$$B_{do1} = -\frac{\hat{F}}{\delta e} \sin\varphi \sin\alpha \sin\theta \tag{23}$$

The maximum e.m.f. is consequently:

$$-\frac{v l}{\theta_{sk}} \frac{A_{q1} \hat{F} \sin\varphi}{\delta e} \int_{-\theta_{sk}/2}^{\theta_{sk}/2} \sin^2\theta \, d\theta = -v l \frac{A_{q1} \bar{F} \sin\varphi}{\delta e} \left\{ \frac{1}{2} - \frac{\sin\theta_{sk}}{2\theta_{sk}} \right\} \tag{24}$$

The reactance corresponding to this component is:

$$\chi_{do1} = \chi'_{aq} \left\{ \frac{1}{2} - \frac{\sin\theta_{sk}}{2\theta_{sk}} \right\} \tag{25}$$

It may be worth-while to note in passing that, since the flux is anti-symmetrically distributed with respect to α , the Fourier coefficient to be used must be A_{q1} and hence this reactance is proportional to χ'_{aq}. On the other hand, the phase of the induced e.m.f. shows that the latter is a direct axis reaction component, and since the current producing this reaction is the direct axis component, certainly this reactance must be a part of the direct axis reactance.

THE QUADRATURE AXIS COMPONENT WITH EVEN SYMMETRY: This component is anti-symmetrical with respect to α , hence yields no flux through the magnet. The maximum reaction e.m.f. occurs when the center of a conductor is at $\alpha = \frac{\pi}{2}$ hence the nature of the m.m.f. is a cross magneti-

zation. Moreover, the current giving rise to this reaction is the quadrature component; therefore the relevant reactance must be a part of the quadrature axis reactance.

The fundamental component of the flux is:

$$B_{qe1} = -\frac{A_{q1}\hat{F}}{\delta_e} \cos\varphi \cos\theta \sin\alpha \tag{26}$$

The maximum e.m.f. in a conductor occurs when the latter is at a position such that $\alpha = \theta + \frac{\pi}{2}$ and is therefore:

$$-\frac{v l}{\theta_{sk}} \frac{A_{q1}\hat{F}}{\delta_e} \cos\varphi \int_{-\theta_{sk}/2}^{\theta_{sk}/2} \cos\theta \sin\left(\theta + \frac{\pi}{2}\right) d\theta$$

$$= -\, v l \frac{A_{q1}\hat{F}}{\delta_e} \cos\varphi \left\{ \frac{1}{2} + \frac{\sin\theta_{sk}}{2\,\theta_{sk}} \right\} \tag{27}$$

The reactance corresponding to this is:

$$\chi_{qe1} = \frac{1}{2} \chi'_{aq} \left\{ 1 + \frac{\sin\theta_{sk}}{\theta_{sk}} \right\} \tag{28}$$

THE QUADRATURE AXIS COMPONENT WITH ODD SYMMETRY: This component is anti-symmetrically distributed with respect to ξ, hence yields no flux through the magnet. Moreover, it has even symmetry with respect to α, so the reaction m.m.f. has a maximum at $\alpha = \frac{\pi}{2}$, hence the nature of this component is a cross magnetization. Furthermore, the current giving rise to this component is the quadrature axis component, and the reactance corresponding to this component must be a part of the quadrature axis reactance.

The fundamental component of flux density is:

$$B_{q01} = -\frac{A_{q1}\hat{F}}{\delta_e} \cos\varphi \sin\theta \cos\alpha \tag{29}$$

The maximum e.m.f. is:

$$-\frac{v l}{\theta_{sk}} \frac{A_{q1} \hat{F} \cos\varphi}{\delta e} \int_{-\theta_{sk}/2}^{\theta_{sk}/2} \sin\theta \cos(\theta + \frac{\pi}{2}) d\theta = \frac{v l \hat{F} \cos\varphi \, A_{q1}}{2\delta e} \left\{ 1 - \frac{\sin\theta_{sk}}{\theta_{sk}} \right\} \tag{30}$$

The relevant reactance is:

$$\chi_{q01} = \chi'_{aq} \left\{ 1 - \frac{\sin\theta_{sk}}{\theta_{sk}} \right\} \tag{31}$$

A FURTHER CLARIFICATION OF THE CONCEPT PERTAINING TO REACTION REACTANCES: Now we have come to the point where a further clarification of the conventional concept of reactances must be made. The armature reaction reactances have been defined by different authors either as "the reactance arising from the armature flux mutual to the rotor winding," or "the reactance arising from the space fundamental of the reaction flux." The implication of the word "reaction" seems to make the former one more adequate. Furthermore, it also has the advantage of a certain degree of consistancy in keeping with the parameters used in the technique of symmetrical components and transient analysis. On the other hand, the latter definition affords easier division of the reactance components. It actually has been elucidated by the Doherty-Nickle's theory, and is satisfactorily consistent with the first definition in the more commonly encountered e.m. cases. The discrepancy arises when all the space fundamental of the flux does not link the rotor winding, as in the case of predominant skewing. When this latter is the case, the components of the flux wave which are anti-symmetrical with respect to the longitudinal coordinate, are definitely leakage in nature. While one has to meet

the difficulty of separating the mutual and the self reactances in making the analysis with unbalanced loading and with transient phenomena, there seems to be no reason for adopting a different point of view in making analysis of a balanced steady state loading. It is the author's opinion that the first definition is more acceptable.

THE MUTUAL FLUX AND THE REACTION REACTANCES: In the analysis for the reaction reactances, the basic fact to be considered is that since the secondary, or the rotor conductors all run in the longitudinal direction and are not skewed, only the components of the space fundamental flux having even symmetry with respect to the longitudinal coordinate are mutual in nature. Since the rotor conductors are unskewed, the integrands yielding the induced voltages have constant values of α , o or $\frac{\pi}{2}$ in the case of direct or quadrature axis reaction respectively. Therefore, the induced voltages are given by:

$$-\frac{vl}{\theta_{sk}}\int_{-\theta_{sk}/2}^{\theta_{sk}/2}\frac{\hat{F}\sin\varphi}{\delta_e}\left\{A'_{d1}\cos\theta-\Pi_o A_{e1}\frac{2}{\theta_{sk}}\frac{\sin\theta_{sk}}{2}\right\}d\theta$$

$$=-\frac{vl\hat{F}\sin\varphi}{\delta_e}\left\{A'_{d1}-\Pi_o A_{e1}\right\}\frac{2}{\theta_{sk}}\sin\frac{\theta_{sk}}{2}=-\frac{vl\hat{F}\sin\varphi}{\delta_e}A_{d1}\frac{2}{\theta_{sk}}\sin\frac{\theta_{sk}}{2} \qquad (32)$$

$$-\frac{vl}{\theta_{sk}}\int_{-\theta_{sk}/2}^{\theta_{sk}/2}\frac{A_{q1}\hat{F}\cos\varphi\cos\theta\,d\theta}{\delta_e}=-\frac{vl\hat{F}\cos\varphi}{\delta_e}A_{q1}\frac{2}{\theta_{sk}}\sin\frac{\theta_{sk}}{2} \qquad (33)$$

for the direct and the quadrature cases respectively. The reaction reactances are then given by:*

$$\chi_{ad}=\chi'_{ad}\left\{1-\Pi_o\frac{A_{e1}}{A'_{d1}}\right\}\frac{2}{\theta_{sk}}\sin\frac{\theta_{sk}}{2}=\frac{A'_{d1}}{A'_{q1}}\frac{2}{\theta_k}\sin\frac{\theta_{sk}}{2}\cdot\chi_{aq'} \qquad (34)$$

$$\chi_{aq}=\chi'_{aq}\frac{2}{\theta_{sk}}\sin\frac{\theta_{sk}}{2} \qquad (35)$$

* When the magnet reluctance is zero and $\chi'_{aq}=\chi_{ad}$ these expressions reduce to a form consistent with Morrill's result for a single phase induction motor.

THE SKEWING REACTANCES: The reactance arising from the entire space fundamental of the reaction flux along either axis has an excess over the corresponding reaction. This excess is leadage in nature and is defined as the skewing reactance. The skewing reactance clearly has different values along the two axes. Their values are given by:

$$\chi_{skd} = \chi'_{ad}\left\{\left(\frac{1}{2}+\frac{1}{2}\,\frac{\sin\theta_{sk}}{\theta_{sk}}\;\;\frac{2}{\theta_{sk}}\sin\frac{\theta_{sk}}{2}\right)+\pi_o\frac{A_{e1}}{A'_{d1}}\frac{2}{\theta_{sk}}\sin\frac{\theta_{sk}}{2}\left(1-\frac{2\sin\frac{\theta_{sk}}{2}}{\theta_{sk}}\right)\right\}+\chi'_{aq}\left\{\frac{1}{2}-\frac{\sin\theta_{sk}}{2\,\theta_{sk}}\right\} \tag{36}$$

$$\chi_{skq} = \chi'_{aq}\left\{\frac{1}{2}+\frac{1}{2}\,\frac{\sin\theta_{sk}}{\theta_{sk}}-\frac{2}{\theta_{sk}}\sin\frac{\theta_{sk}}{2}\right\}+\chi'_{ad}\left\{\frac{1}{2}-\frac{1}{2}\,\frac{\sin\theta_{sk}}{\theta_{sk}}\right\} \tag{37}$$

As shown by these expressions for the reaction and the leakage reactances, when the reluctance of the magnet is zero and the poles are non-salient, the effect of skewing is to subtract a part from the reactance and to add the same to the leakage reactance, leaving the total reactance unchanged. When this is not the case, the general trend is the same but the total reactances are in general different from the unskewed values, and also a leveling effect between the two reactances occurs.

EFFECT OF SKEWING UPON THE SLOT AND THE DIFFERENTIAL LEAKAGE REACTANCE: Skewing the armature slots has an effect of increasing the apparent length of the conductors embedded in the slots and diminishing the width of the slots; both in turn increase the slot reactance. The increase is thus twofold, and is proportional to the square of the secant of the physical angle of skew. Hence, the slot reactance must be multiplied by a factor:

$$1 + \left(\theta_{sk} D / \eta_p l \right)^2 \qquad \theta_{sk} \text{ in Radians.} \tag{38}$$

The differential reactances are apparently little affected by skewing.

IV EXPERIMENTAL CONFIRMATION

The formulae presented in this report have been used to calculate the reactances of two existing p.m. alternators made by O'Keefe and Merritt Company. Since there are difficulties not overcome in direct measurement of the reactances of the p.m. alternators, the regulation curves calculated from these reactances have been compared with test data supplied by the manufacturer, to yield an indirect indication of the accuracy of the theory.

One machine on which the check has been made is the O'Keefe and Merritt Model MG-15-400, rated at:

3 ph.	400 cps	120/208 ph./line volts
15 KW at	0.8	1714 rpm 28 poles
No load phase voltage		124 v.

The calculated constants are:

$A_{di}' = 0.0944$ $A_{ei} = 1.245$ $\pi_o = 0.622$
$A_{di} = 0.219$ $A_{qi} = 0.626$ $\chi_m = 1.74$ Ohms
$\theta_{sk} = \pi/3$ $\sin\theta_{sk}/\theta_{sk} = 0.827$ $R_a = 0.069$ Ohm

$\sin(\theta_{sk}/2)/\theta_{sk}/2 = 0.955$ $A_{ei}/A_{di}' = 1,253$

$\chi_{ad} + \chi_{skd} = 0.441$ Ohm
$\chi_{aq} + \chi_{skq} = 1.131$ Ohm
$\chi_s = 0.188$ Ohm
$\chi_e = 0.018$ Ohm
$\chi_z = 0.120$ Ohm
$\chi_b = 0$ Ohm
$\chi_d = 0.771$ Ohm
$\chi_q = 1.464$ Ohm

Because of the low flux density used in this machine, the load saturation effect is not predominant. Consequently, the two reactance method has attained a very satisfactory accuracy. As shown in Fig. 10, the test point at zero power factor lagging is almost exactly on the calculated curve. The check at unity factor is also within 2.5%, based upon the no load voltage as 100%.

The other machine checked is the O'Keefe and Merritt Model PU-31, rated at:

3 ph.	60 cps	120/208 v.ph./line
5 KW at	0.8	1800 rpm 4 poles
No load ph.v.		121 v.

The skewing employed in this machine is rather small. The calculated constants are:

$A_{d1} = 0.120$	$A_{q1} = 0.208$
$\chi_l = 0.208$ ohm	$R_a = 0.170$ ohm
$\chi_{ad} = 1.926$ ohm	$\chi_{aq} = 7.52$ ohm
$\chi_a = 2.134$ ohm	$\chi_q = 7.73$ ohm

The regulation curves for this machine are shown in Fig. 11. The calculated curve for the zero power factor lagging again checks closely with the test points. Because of the higher flux density employed in this machine, the load saturation effect at the teeth has a large influence upon the regulation. The rising trend of the theoretical curve for unity p.f. which is a result of the much greater value of χ_q over χ_d, is more than offset by the saturation effect. The discrepancy is about 13% in the worst part of the curve, based upon no-load voltage as 100%.

V CONCLUSION

From the foregoing discussions and the experimental confirmation, it may be concluded that, whenever saturation effect is not excessive, the formulae developed in this report yield a satisfactory calculation of the

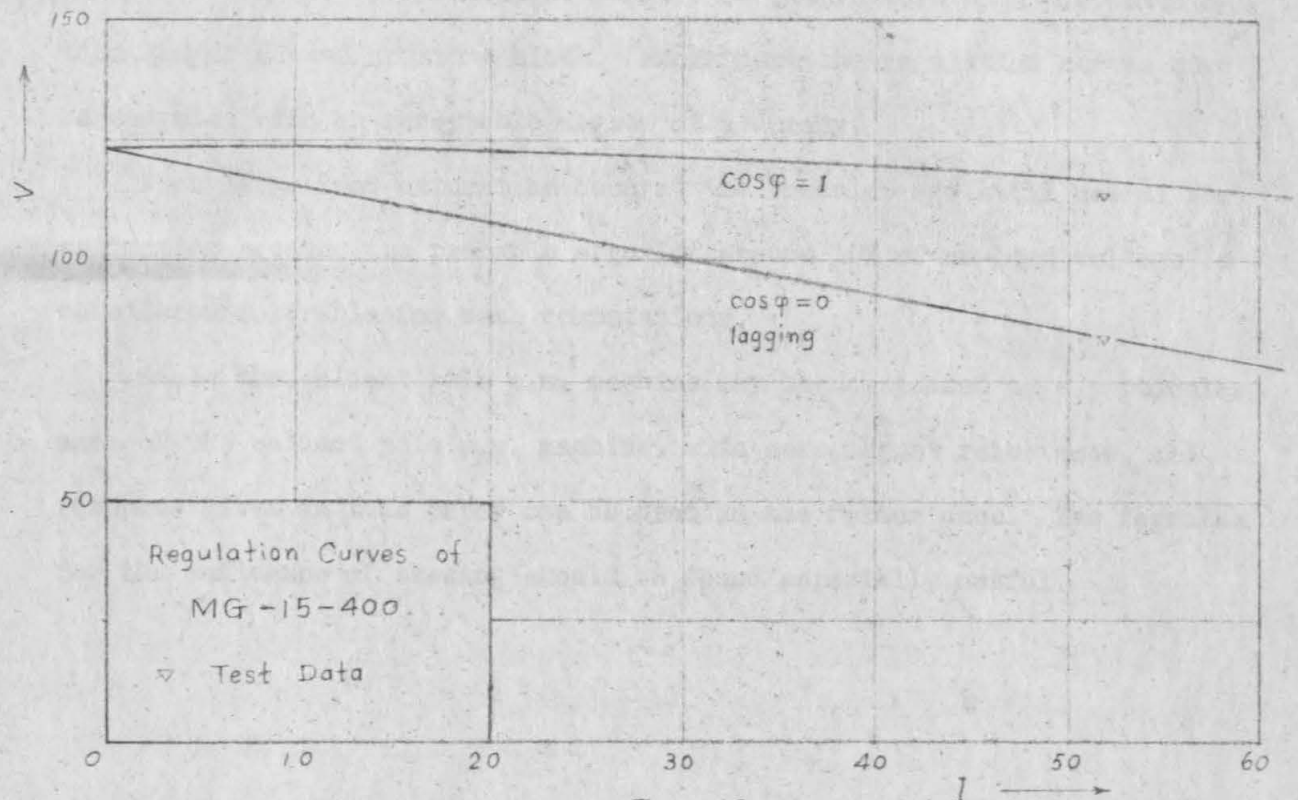
150
V
100
50
cosφ = 1
cosφ = 0
lagging
Regulation Curves of
MG-15-400
▽ Test Data
0
10
20
30
40
50
60
I

FIG 10

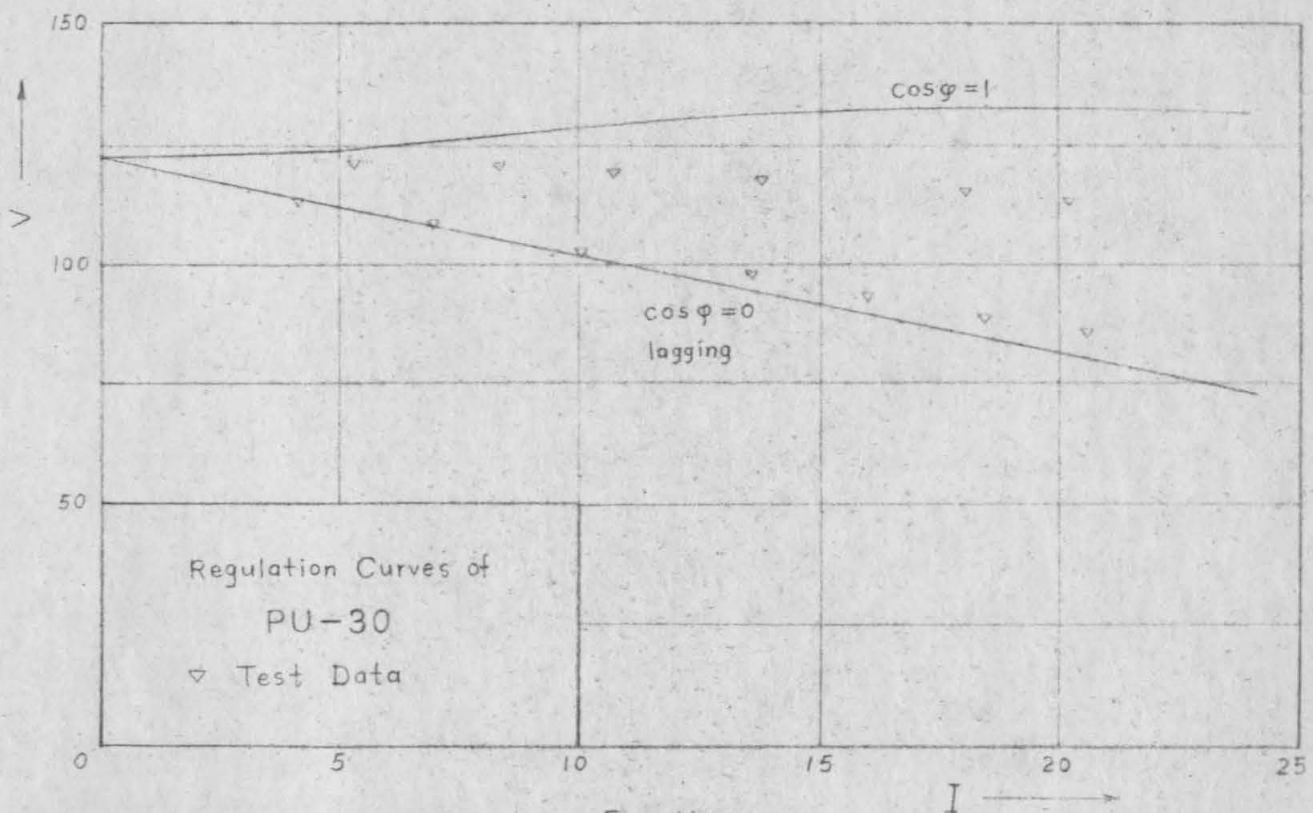
150
V
100
50
cosφ = 1
cosφ = 0
lagging
Regulation Curves of
PU-30
▽ Test Data
0
5
10
15
20
25
I

FIG 11

values of the two synchronous reactances of alternators with p.m. excitation and/or skewed armature slots. From these the regulation curves may be computed with an acceptable degree of accuracy.

When large load saturation occurs, the formulae are still useful for estimation because the probable error of around 10% of no-load voltage is considered tolerable for such computations.

Since the salient pole e.m. machine may be considered as a particular case of the salient pole p.m. machine, with zero magnet reluctance, all formulae given in this paper can be used in the former case. The formulae for the influence of skewing should be found especially useful.

APPENDIX I

FLUX PLOTTING IN PRESENCE OF PERMANENT MAGNETS

The rules for magnetic flux plotting as laid down by Doherty and Shirley for e.m. excited machines must be augmented in two respects when permanent magnets are present.

Firstly, in the armature reaction plot, the field produced by the permanent magnetization having been removed from the total field, all the flux lines crossing the boundaries of the magnets must be plotted according to the following rules:

(1) Across a magnet-iron boundary, the flux lines must be normal to the boundary line, and

(2) Across a magnet-air boundary, the flux lines must be refracted:

$$\frac{\tan\theta_m}{\tan\theta_a} = \frac{\mu_\Delta}{\mu_o} = K_\Delta \qquad (39)$$

where the angles are defined in Fig. 12.

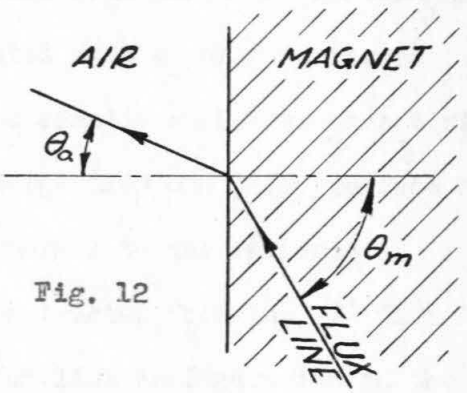

Fig. 12

Secondly, the rules for plotting the field due to the permanent magnetization are set forth in the following manner:

The magnetization in a magnet, aside from the influence of any external m.m.f., is composed of two parts, viz., a permanent part M_o and an induced part M'. The fundamental relation in the field is:

$$B = \mu_o(H + M) = \mu_o(H + M' + M_o) = \mu_\Delta H + \mu_o M_o \qquad (40)$$

where $\mu_o M_o$ is the same as the conventional intrinsic induction. Taking the divergence of both sides:

$$\text{div}\,(\mu_\Delta H) = -\,\text{div}\,M_o = \rho_m \quad , \tag{41}$$

which shows that the vector field of $\beta = \mu_\Delta H$, which is here defined as a lamellar induction vector, can be derived from a scalar potential satisfying Poisson's equation.

From this, each magnet in a salient pole alternator, being rectangular in shape and nearly magnetized uniformly along one normal direction, may be replaced by:

(1) A bulk of paramagnetic material with the same configuration and a permeability μ_Δ , and

(2) A surface source and a surface sink with strengths numerically equal to the permanent magnetization, located at the polar surfaces.

Thus, the β-flux lines can be plotted exactly as B-flux except with one additional rule: All β-flux lines emerge from one polar surface and submerge into the other along a direction normal to the surfaces.

Although the B-flux lines can be reconstructed from the β-flux lines, this is scarcely necessary since only B-flux line configuration in the air is interesting to the designer and this is the same as the one for the β-flux. Also, it is apparent that the B-plot shown in Fig. 3 is exactly the same as the β-plot for the case when the excitation is acting alone.

APPENDIX II

SYMBOLS AND DEFINITIONS

A_{do} Ratio of average air gap flux density produced by direct axis armature reaction to the peak value.

A'_{do} The same with zero magnet reluctance.

A_{d1} Ratio of maximum value of the space fundamental of the direct axis armature reaction flux density to the peak value.

A'_{d1} The same with zero magnet reluctance.

A_{q1} Ratio of the maximum value of the space fundamental of the quadrature axis armature reaction flux density to the hypothetical peak value. (See text.)

A_{eo} Ratio of the average excitation flux density to the peak value.

A_{e1} Ratio of the maximum value of the space fundamental of the excitation flux density to the peak value.

B_{de1} Component of the direct axis flux density due to the space fundamental, having even longitudinal symmetry.

B_{do1} The same with odd symmetry.

B_{qe1} Component of the quadrature axis flux density due to the space fundamental, having even longitudinal symmetry.

B_{qo1} The same with odd symmetry.

D Diameter at the air gap.

E Induced e.m.f.

E' Unskewed induced voltage in a skewed conductor.

F Armature reaction magnetomotive force.

$\hat{F}$ Maximum value of the space fundamental of the armature reaction m.m.f.

F_{de} The component of armature reaction m.m.f. arising from the space fundamental of the direct axis armature current distribution, with even longitudinal symmetry.

F_{do} The same with odd longitudinal symmetry.

F_{qe} The same for quadrature axis current, with even longitudinal symmetry.

F_{qo} The same for quadrature axis current, with odd longitudinal symmetry.

M_o Permanent part of the magnetization.

f_b The form factor of the excitation flux distribution.

f_c The pitch factor of the winding.

f_d The distribution factor of the excitation flux distribution.

f_w The breadth factor of the winding.

H The magnetic field intensity.

M Magnetization in the magnet.

l The length of the armature.

m The number of phases.

N Number of conductors in the armature winding.

n_p Number of poles.

N_{psd} Number of squares along a tube of force between the pole face and the armature surface at the center of the pole in a direct axis flux plot.

N_{tfd} Number of squares along the whole periphery of the pole piece in a direct axis flux plot.

N_{psf} Number of squares along a tube of force between the pole face and the armature surface in an excitation flux plot.

N_{tfe} Number of squares along the whole periphery of the pole piece in an excitation flux plot.

v Periphery velocity of the rotor.

χ_{ad} Direct axis armature reaction reactance.

χ_{aq} Quadrature axis armature reaction reactance.

χ_{d1} Direct axis reactance arising from the space fundamental of armature flux.

χ_{q1} Same for quadrature axis.

χ_{de1} Reactance arising from B_{de1}.

χ_{do1} Reactance arising from B_{do1}.

χ_{qe1} Reactance arising from B_{qe1}.

χ_{qo1} Reactance arising from B_{qo1}.

χ_{sk} Skewing reactance.

α Angular position of the center of a conductor recognized from the center of the pole, electrical degrees.

β The lamellar magnetic induction vector.

θ The angular position of an infinitesimal element of conductor recognized from the angular position of the center of the conductor as zero, electrical degrees.

θ_{sk} The angle of skew in electrical degrees.

δ_e Effective length of air gap.

φ Phase angle between the resultant open circuit voltage and the load current.

μ_Δ Incremental permeability of the permanent magnet material.

μ_o Permeability of the vacuo.

ξ Longitudinal position of an infinitesimal element of a conductor.

π_o Ratio of the magnetic potential of the pole piece produced by the direct axis armature reaction magnetomotive force to the maximum value of the latter in the absence of skewing.

ρ_m Equivalent magnetic charge density of the permanent part of the magnetization.

REFERENCES

1. Alger, P. L., Calculation of Armature Reactances of Synchronous Machines, Trans. A.I.E.E. (1928) Vol. 47, p. 493.

2. Kilgore, L. A., Calculation of Synchronous Machine Constants, Trans. A.I.E.E. (1931) Vol. 50, pp. 1201-1213.

3. Kilgore, L. A., Effect of Saturation of Machine Reactances, Trans. A.I.E.E. (1935) Vol. 54, pp. 545-550.

4. Langsdorf, Theory of Alternating Current Machinery, (a book) pp. 371-380, McGraw-Hill, New York.

5. Doherty and Nickle, Synchronous Machines I, Trans. A.I.E.E. (1926) Vol. 45, p. 912.

6. Morrill, Characteristic Constants of Single Phase Induction Motors, Part I, Trans. A.I.E.E. (1937) Vol. 56, p. 333.

7. Bewley, L. V., Induced Voltages of Electrical Machines, Trans. A.I.E.E. (1930) Vol. 49, pp. 450-468.

8. Sah, P.T., Fundamentals of Alternating Current Machines, (a book) first edition (1946) p. 231, McGraw-Hill, New York.

9. Appendix of Stevenson and Park, Graphical Determination of Magnetic Fields, Trans. A.I.E.E. (1927) Vol. 46, p. 136.

PART II

THE CARDIOID DIAGRAM METHOD

THE CARDIOID DIAGRAM METHOD OF DETERMINING THE VOLTAGE REGULATION OF SALIENT POLE ALTERNATORS AND THE LOAD VOLTAGE EXALTATION PHENOMENON IN ALTERNATORS WITH PERMANENT MAGNET EXCITATION

I THE CARDIOID DIAGRAM METHOD

The Diagram: The cardioid diagram method of determining the voltage regulation of an alternator is only a special application of polar diagram methods which is especially convenient for working with the two reaction theory.

In Fig. 1, a vector diagram is shown for a permanent magnet alternator under a lagging power factor load. The open circuit voltage E leads the load current I by an angle φ. The terminal voltage V leads the current by an angle ϑ. E differs from V by the vector sum of the three voltage drops IR, $jI_d X_d$, and $jI_q X_q$. Since X_q is much greater than X_d, $I_q X_q$, is also greater than $I_d X_d$ except at nearly zero power factor.

Now, a vector perpendicular to IR is drawn from the head of the latter, intersecting the extended E vector at point C. Clearly this new vector is equal to jIX_q, since its magnitude is $I_q X_q / \cos\varphi = IX_q$ and it is in the right direction. The fictitious voltage E' differs from E by $I_d(X_q - X_d)$.*

---

* In a p.m. alternator, X_q is in general greater than X_d. See "The Synchronous Reactances of Alternators with Permanent Magnet Excitation and Alternators with Skewed Armature Slots" by the same author.

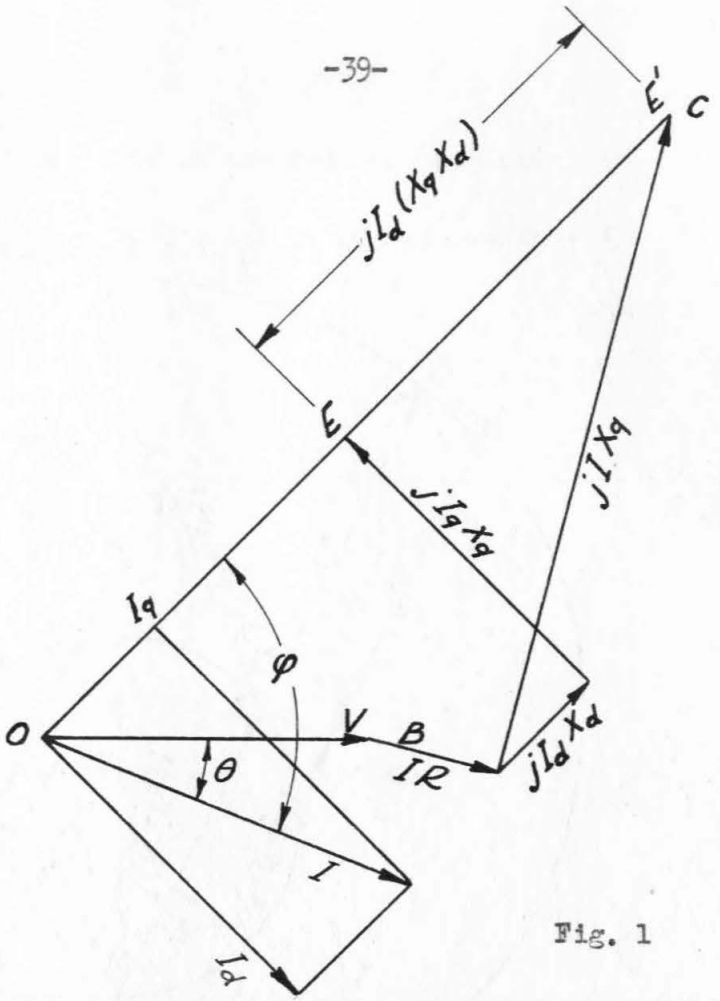

Fig. 1

This relation can be represented by the equation:

$$V + IR + jIX_q = E' = E + jI\cos\varphi\,(X_q - X_d) \qquad (1)$$

Now, consider a permanent magnet alternator. The open circuit voltage E, and the rated load current I are given, and the voltage at any power factor is required. First of all, as shown in Fig. 2, the coordinate axes are rotated such that the real axis coincides with I. A circle is then drawn passing through O, with center on the imaginary axis and with diameter equal to $I(X_q - X_d)$. Any radius vector terminating on this circle, inclined at an angle to the real axis, say OA, represents $jI\cos\varphi\,(X_q - X_d)$. Each such vector, when extended by a length E, then represents E'.

The locus of E′ lies on the rotated cardioid:

$$\text{radius } R = E' = I(\chi_q - \chi_d)\cos\varphi + E \qquad (2)$$

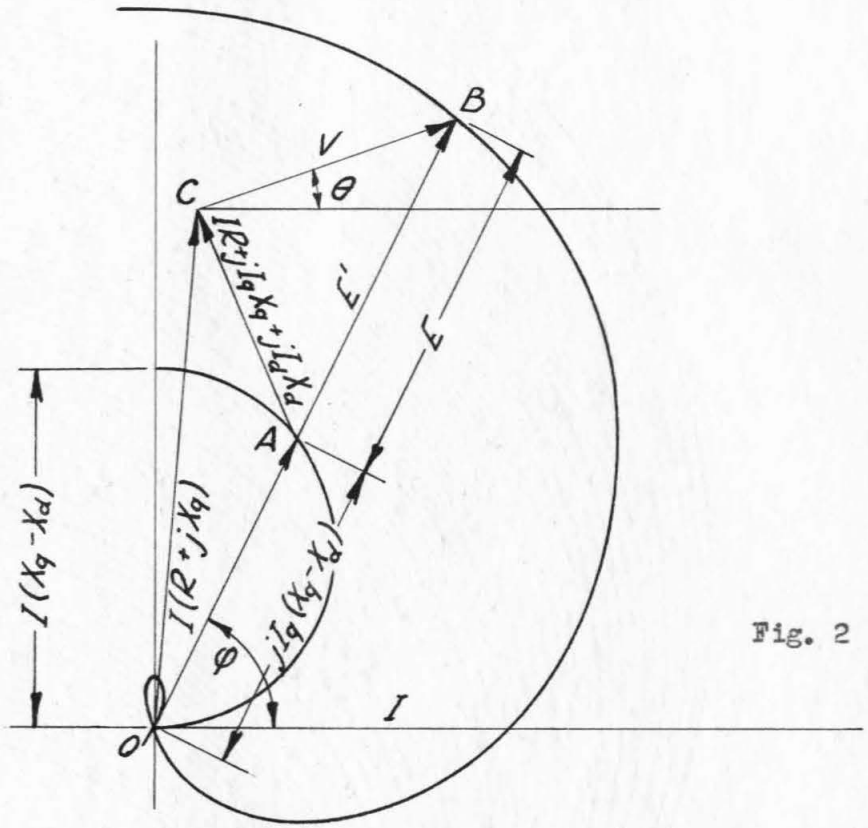

Fig. 2

There is thus a cardioid for each value of $I(\chi_q - \chi_d)$ and hence for each I .

Then a vector representing $I(R + j\chi_q)$, OC, is erected upward from the origin. From C, a vector is drawn at an angle ϑ to the real axis, terminating at a point B, on the cardioid. This vector, then, represents the terminal voltage V , for this power factor angle ϑ , since it satisfies the relation (1).

II UNIVERSAL CARDIOID GRAPH PAPER

Since the cardioids are relatively simple curves and can be constructed with ease, use can be made of a cardioid graph paper. On this graph paper, a large group of cardioids are drawn with unity E , each corresponds to a PU value of $I(\chi_q - \chi_d)$ based upon E . To use this paper,

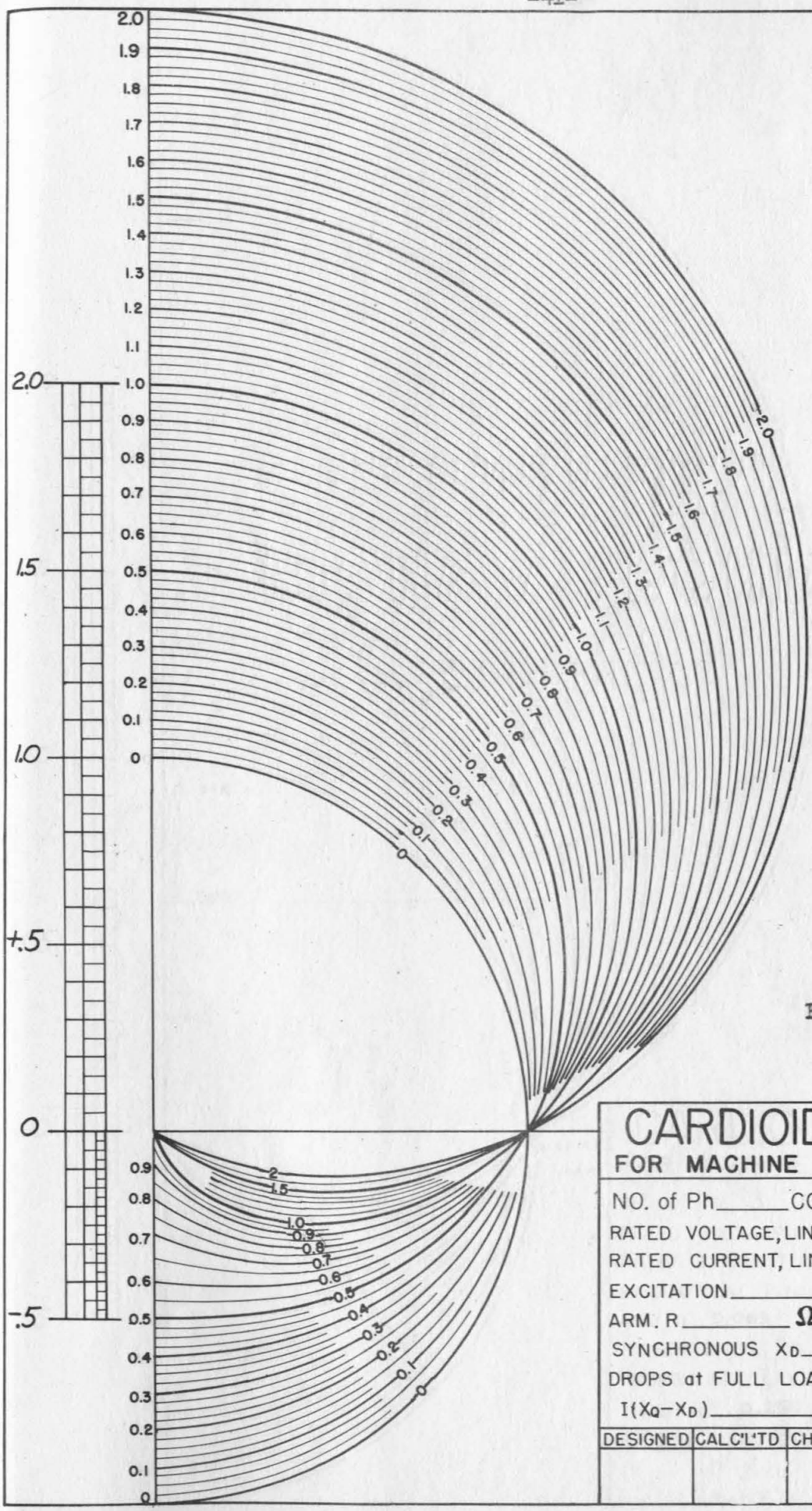

Fig. 3

CARDIOID DIAGRAM

FOR MACHINE MODEL _____

NO. of Ph_____ CONNECTION_____ FREQ_____

RATED VOLTAGE, LINE_____ Ph_____

RATED CURRENT, LINE_____ Ph_____

EXCITATION_____ NO LOAD V_____

ARM. R_____ Ω, LEAKAGE X_____ Ω

SYNCHRONOUS X_D_____ Ω X_Q_____ Ω

DROPS at FULL LOAD, PU of NO LOAD V

$I(X_Q - X_D)$_____ $I(R + jX_Q)$_____

DESIGNED	CALC'L'TD	CHECKED	APPROVED

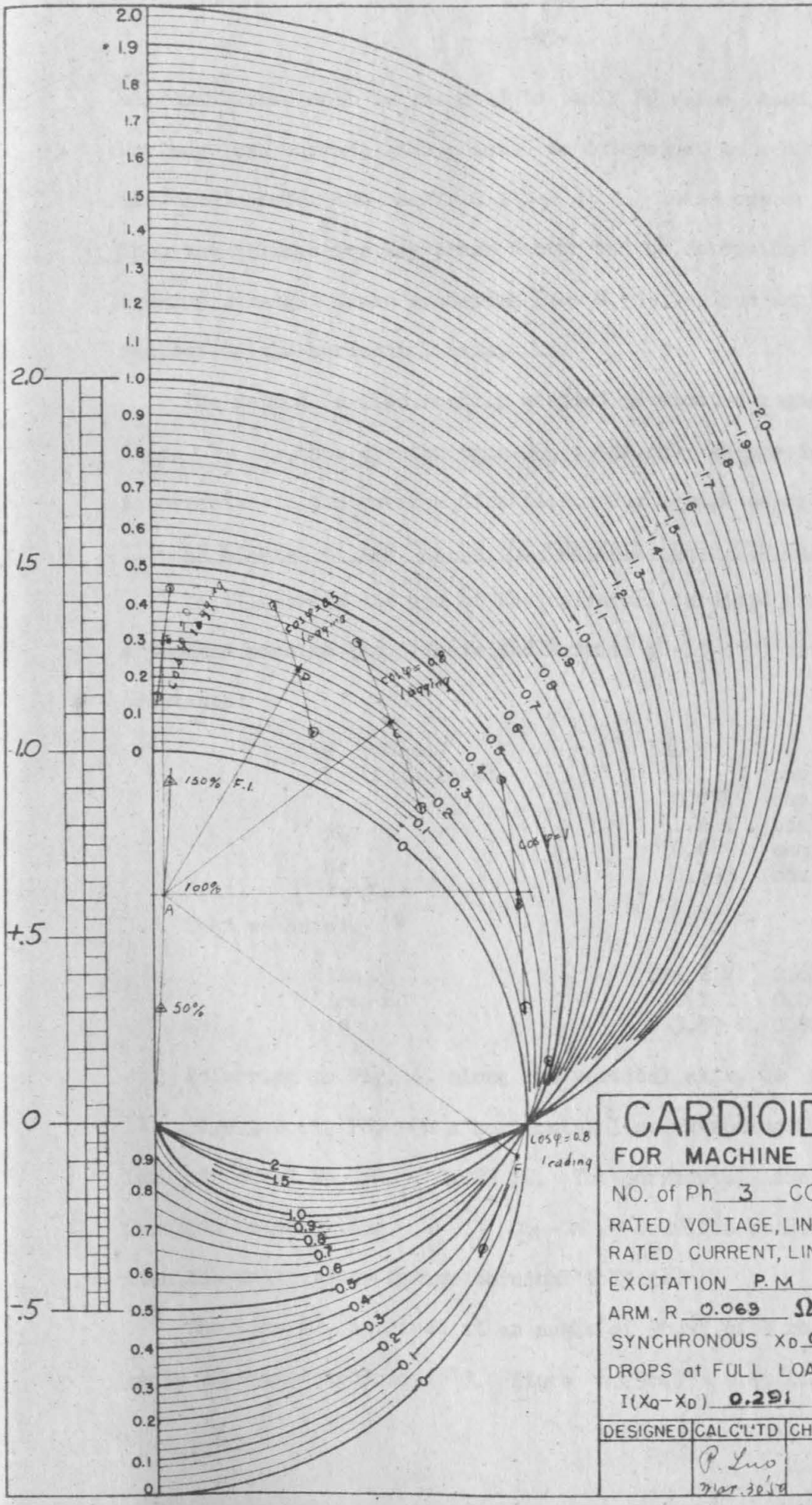

Fig. 4

x Full Load.

CARDIOID DIAGRAM

FOR MACHINE MODEL MG 15-400

NO. of Ph 3 CONNECTION Δ/Y FREQ 400

RATED VOLTAGE, LINE 120/208 Ph 120 V

RATED CURRENT, LINE 90.2/52.1 Ph 52.1 A

EXCITATION P.M NO LOAD V 124

ARM. R 0.069 Ω, LEAKAGE X _____ Ω

SYNCHRONOUS X_D 0.771 Ω X_Q 1.464 Ω

DROPS at FULL LOAD, PU of NO LOAD V

$I(X_Q - X_D)$ 0.291 $I(R+jX_Q)$ 0.029+j0.614

DESIGNED	CALC'L'TD	CHECKED	APPROVED
	P. Luo Mar. 30/'70		

all quantities must be computed to their PU value based upon E as unity. For any load current, the point C is determined as mentioned above, and the cardioid for the required $I(\chi_q-\chi_d)$ is picked out or interpolated. Then the voltage for any power factor can be determined immediately by drawing straight lines radiating from C, at various angles, ϑ , with respect to the horizontal axis.

The method is also readily adapted to electro-magnetic alternators. Since χ_d is then greater than χ_q , the only change is that the paper is oriented in the reverse direction. Such graph paper is shown in Fig. 3.

III AN EXAMPLE OF THE USE OF THE UNIVERSAL CARDIOID GRAPH PAPER

To illustrate the use of the universal cardioid graph paper, consider a 3-phase machine (an O'Keefe and Merritt MG-15-400) with the following constants:

E (phase)	124 V	
I (full load)	52.1	amp
χ_d	0.771	ohm
χ_q	1.464	ohm
R_a	0.069	ohm
$\chi_q-\chi_d$	0.693	ohm

Then we have:

$I\chi_q$	76.2 V	0.614 PU
$I(\chi_q-\chi_d)$	36.1 V	0.291 PU
IR	3.59 V	0.029 PU

Referring to Fig. 4, along the vertical axis, OA′ is laid off equal to $I\chi_q$, i.e., 0.614 PU. On a horizontal line extending from A′ , A′A is laid off equal to IR_a , 0.029 PU. The horizontal line AB intersects the cardioid representing $I(\chi_q-\chi_d) = 0.291$ PU at B. The vector AB is then the unity power factor terminal voltage.

The line AC, inclined at an angle of 36.9° with respect to AB, intersects the same cardioid at C. Since $\cos 36.9° = 0.8$, AC is the terminal

voltage for 0.8 power factor lagging. By a similar procedure, the terminal voltage can be obtained for any power factor and any load. In Fig. 4, points similar to A for different loads are marked with small triangles. The points corresponding to B, C, D, and E are marked with small circles. Lines connecting these points are omitted to avoid confusion.

IV THE LOAD VOLTAGE EXALTATION PHENOMENON IN ALTERNATORS WITH PERMANENT MAGNET EXCITATION

While in the electromagnet excited alternators the terminal voltage rises with load current highly capacitive, in certain permanent magnet excited machines, the same phenomenon has been observed with load current of unity power factor. Actually, this load voltage exaltation phenomenon may be proved to occur over wide range of power factor, from purely capacitive through unity factor, to somewhat inductive. This phenomenon has been attributed to the unusual combination in permanent

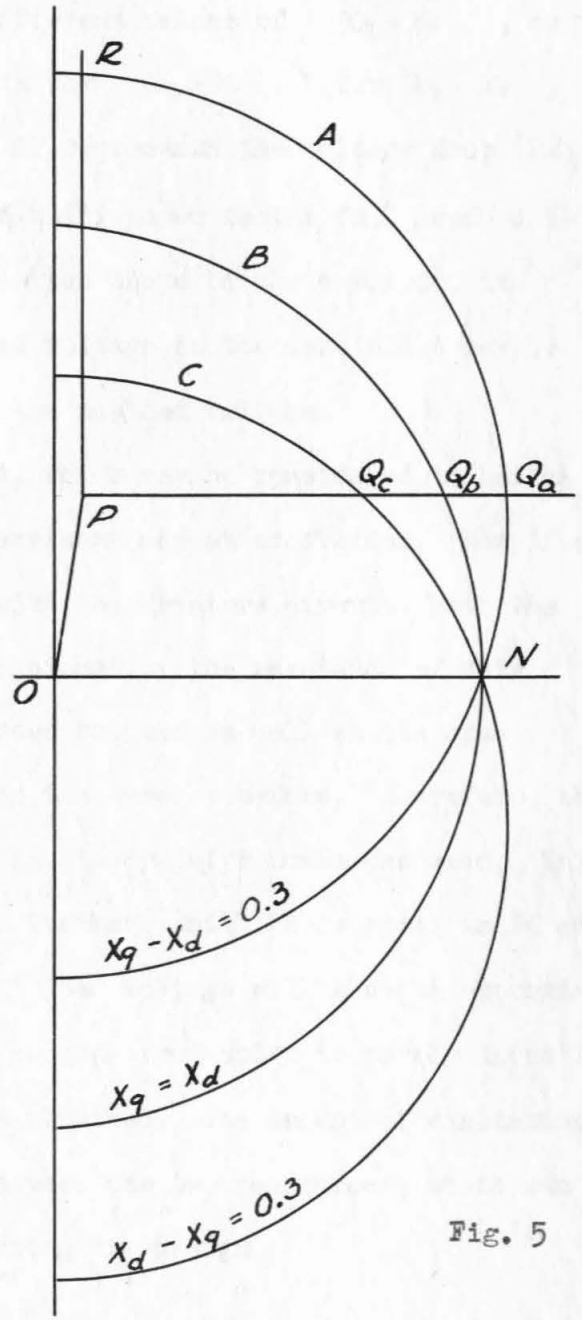

Fig. 5

magnet machines of smaller χ_d and greater χ_q . By means of the cardioid diagram, this may be explained and, furthermore, this phenomenon may be shown to be useful in obtaining a system with rising regulation curve uniform over a range of power factor from unity to purely inductive. This latter possibility is indeed very desirable as an expedient to combat the line drop.

Consider the cardioids for different values of $\chi_q - \chi_d$, as shown in Fig. 5. The cardioid A is for $\chi_q > \chi_d$, B for $\chi_q = \chi_d$, and C for $\chi_q < \chi_d$. The vector OP represents the voltage drop IZ_q so PQ_a, PQ_b, and PQ_c represent the unity power factor full load voltages for the three cases. Owing to the shape of the cardioid, it becomes apparent that the full load voltage on the cardioid A may be greater than ON, which represents the no-load voltage.

Again consider the cardioid A, which may be considered to be the one for a specific machine with permanent magnet excitation. Now if a capacitor is connected in series with the armature circuit, both the reactances χ_d and χ_q will be diminished by the reactance of this capacitor, but the difference between the two as well as the open circuit induced voltage will remain the same as before. Therefore, the cardioid diagram will be the same but the point P moves downward. This process can be carried further and further, until PR is equal to PQ and both are greater than ON. The full load voltage will then be approximately constant for power factors ranging from unity to purely inductive. Thus the desired characteristic is obtained. The amount of exaltation is determined by the difference between the two reactances, which can be controlled within certain range during the design.

The load exaltation, as described in this section, can be fully realized only when saturation is absent. As stated in a paper by the same author,* the load saturation effect prevailing in certain p.m. alternators reduces the χ_q and likewise $\chi_q - \chi_d$. This tends to reduce the amount of load voltage exaltation.

V CONCLUSION

The cardioid diagram method greatly simplifies the work of calculating the regulation of salient pole alternators for wide range of loads and power factors. At such low flux density that the reactances may be considered constant, if a sufficiently large scale is used, the accuracy of this method can meet the requirement for most practical purposes.

Since saturation effect is less serious in p.m. excited alternators than in e.m. excited ones, this method is found especially useful with the former. When saturation cannot be neglected, it is still useful if the saturated values of the reactances are known.

By means of a study of the cardioid diagram, it has been found to control the load voltage exaltation phenomenon in certain p.m. excited alternators to produce a uniformly rising regulation curve over a wide and useful range of power factor.

---

* Loc. cit.

PART III

THE OPTIMUM PROPORTIONS OF THE FIELD STRUCTURE OF PERMANENT MAGNET EXCITED ALTERNATORS

THE OPTIMUM PROPORTIONS OF THE FIELD STRUCTURE OF PERMANENT MAGNET EXCITED ALTERNATORS

I GENERAL

1-5

INTRODUCTION: Several important articles have appeared in the past few years to discuss the most economic proportions of permanent magnets both under constant and under variable working conditions. In all these articles, however, the magnets have been considered, to certain extent, separate from the rest of the system. Hence, the conclusions have been very general but rather indefinite. When all constraints arising from the connected systems are considered for a particular type of problem, the optimum design must be very definite in nature. The purpose of this paper is to present the solution of a class of problems typified by permanent magnet excited alternators.

A problem of such a class in general falls into either of the following two types:

(1) With the diameter of the rotating field structure fixed, what could be the maximum attainable air gap flux density, and what would be the optimum dimensions to yield this?

(2) If the air gap flux density is specified, what would be the optimum dimensions giving rise to a minimum weight of the magnets?

In either type, the requirement as to the stability and the length of the air gap must be prescribed.

SPECIFICATION OF THE STABILITY: Since the rotors of salient pole machines with permanent magnet excitation are either provided with heavy damping windings or are cast into solid aluminum structures, electric transient demagnetization is usually sufficiently damped so as to be

negligible. Among the remaining possibilities, two major types may be mentioned: (1) Sustained short-circuit or overload of a nature determined by the type of the intended service, and (2) short-time overload due to mechanical transients such as the starting of motors. In both cases the power factors are likely to be low and inductive.

A quantity, the voltage stability factor, has been found convenient for design analysis and for ease in planning a machine for some given service requirement. This is defined as the maximum allowable voltage drop, based upon the open circuit voltage as unity, the machine can stand under pure inductive load current without impairing the magnets. As will be seen later, this factor does not enter directly into the results. Instead, the one to appear explicitly is a factor ϵ_s, the normalized value of the equivalent permeance external to the rotor when the machine is working at the point of stabilization. The forthcoming analyses are sufficiently general to allow their utilization whenever the value of ϵ_s can be estimated.

ESTIMATION OF ϵ_s : Sometimes the magnets are stabilized by putting the rotor out into open space after the initial magnetization. In this case, the value of ϵ_s may be estimated from a flux plot or by conformal transformation method, or anything else available in the potential theory. However, in most practical applications, the stability so obtained will be far more than necessary.

The method of stabilization to be recommended is then to bring the working point of the magnets to the intended point of stabilization after initial magnetization and final assembly, say, by applying an inductive overload current of proper magnitude for a very short time.

The value of the factor ϵ_s can be computed from the voltage stability factor with the following formula:

$$\epsilon_s = 1 - \frac{\nu A'_{do} A_{e1}}{A_{eo} A'_{d1} + \frac{\chi_{ld}}{\chi_m} - (1-\nu)\frac{A'_{do} A_{e1}}{1 + \lambda + \mu_a m}} \qquad (1)$$

Unless ν is very small, the variation of ϵ_s with λ and m is rather slow so ϵ_s will be considered independent of the latter factors in the following analyses. Also, the value of $\frac{\chi_{ld}}{\chi_m}$ is rather small as compared with the whole denominator, so may be neglected in preliminary computations.

THE LENGTH OF THE AIR GAP: For a minimum weight of the magnets, the air gap must be as short as mechanical limits will permit. Although the reactance may be a limiting factor, by far the most important restriction in practice is the difficulty in maintaining a close tolerance and small eccentricity.

SIMPLIFICATION OF THE PROBLEM: In order to render the analysis both useful and practical, the following simplifications have been made:

(1) End fringing effect considered negligible, so the problem may be considered a two-dimensional one.

(2) The representation of the parts of the demagnetization curve above the knee and below the knee by separate straight lines.

(3) The minor loop linear and reversible.

II THE OPTIMUM PROPORTION FOR MAXIMUM AIR GAP FLUX DENSITY

THE MAGNETIC CONSTRAINT: Referring to the demagnetization curve shown in Fig. 1, when a magnet is properly magnetized and stabilized, the operating point will always be on the minor SW where S is the point of stabilization, which must correspond to the maximum demagnetization to which the magnet is to be subjected under the most severe working condition. At this point S, the equivalent external permeance is defined as the ratio of the total flux emerging from the pole face to the scalar magnetic potential of the pole piece. The total permeance in the external magnetic circuit is then composed of this equivalent permeance $\epsilon_s p_g$ and the internal leakage permeance λp_g in parallel. On the other hand, under normal open circuit condition, this is composed of the air gap permeance in parallel with the same internal leakage permeance.

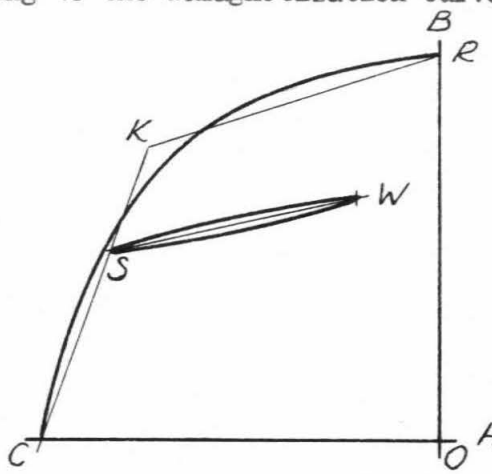

Fig. 1

If the $\lambda + \epsilon_s$ is low the point S will be low and likewise the available flux density in the air gap, under normal open circuit condition. If λ is too high, much flux will be diverted into the internal leakage under open circuit condition. Since both lead to zero air gap flux density when carried to the extremes, there is apparently a maximum for a certain value of λ .

In other words, when the internal leakage is of proper magnitude, it has a beneficial effect of protecting the magnet from excessive demagnetization, so it will be referred to as the protective leakage.

THE DIMENSIONAL CONSTRAINT: In the rotor of an alternator, the size of a magnet is confined to a pole sector subtending an angle $\frac{2\pi}{n_p}$, less the space occupied by the pole piece. Furthermore, the protective leakage is usually provided at the pole tips, so the latter must have a radial depth sufficient to carry the flux allotted to it without appreciable saturation at the point of stabilization. Therefore, the depth of the pole piece must be proportional to the pole width of the magnet. When all these factors are taken into account, there is apparently an optimum magnet width. For any magnet wider than this, the magnet will be too short in the direction of flux and the magnetomotive force from it will be too small. For any magnet narrower than the optimum, the cross sectional area will be too small and the total flux will also be small. The maximum amount of the flux, and hence the maximum air gap flux density, is only obtained at this optimum width. The dimensional constraint determines an optimum proportion of the magnet for any specific value of λ.

For a very large air gap, the optimum point of stabilization will be below the knee. For a very small air gap, it will be above the knee. For a practical air gap length, the optimum point is right at the knee. This is a very important case in practice. This argument can be made clear by the following detailed considerations.

STABILIZATION ON THE LOWER PART OF THE DEMAGNETIZATION CURVE: This part of the demagnetization curve may be approximated linearly by:

$$B = B_{rl} + \mu_l H \qquad \text{- - - - - (2)}$$

The peak value of the air gap flux density is, for any values of λ and m :

$$\hat{B}_g = \frac{(1+2\tau)\left(1+\frac{\mu_\Delta}{\epsilon_s+\lambda}m\right)}{(1+\lambda)\left\{A_{eo}\frac{\pi}{\eta_p}\left(\cot\frac{\pi}{\eta_p}+\sigma\right)+\frac{2\Delta}{m}\right\}\left(1+\frac{\mu_1}{\epsilon_s+\lambda}m\right)\left(1+\frac{\mu_\Delta}{1+\lambda}m\right)} \qquad -----(3)$$

If both σ and ϵ_s are considered independent of λ and m , the optimum value of λ (obtained by what process) under the mentioned constraints is; for any value of m :

$$\lambda_{opt} = \sqrt{\{(1+\epsilon_s)(\mu_1-\mu_\Delta)m\}} - \mu_\Delta m - \epsilon_s \qquad -----(4)$$

With the optimum value of λ , an optimum value of m is found to yield an absolute maximum:

$$m_{opt} = \left\{\frac{2\Delta}{A_{eo}}\frac{1}{\frac{\pi}{\eta_p}\left(\cot\frac{\pi}{\eta_p}+\sigma\right)}\right\}^{2/3}\left\{\frac{1-\epsilon_s}{\mu_1-\mu_\Delta}\right\}^{\frac{1}{3}} \qquad -----(5)$$

The corresponding value of $\hat{B}_g$ at open circuit is:

$$B_{gopt} = \frac{1-2\tau}{1-\epsilon_s}\frac{B_{r1}}{\left\{\left[A_{eo}\frac{\pi}{\eta_p}\left(\cot\frac{\pi}{\eta_p}+\sigma\right)\right]^{\frac{1}{3}}+\left[2\Delta\frac{\mu_1-\mu_\Delta}{1-\epsilon}\right]^{1/3}\right\}^3} \qquad -----(6)$$

The point of stabilization on the demagnetization curve is then:

$$H_{nopt} = -\frac{1}{\mu_1-\mu_\Delta}\frac{B_{r1}}{1+\left[\frac{A_{e1}}{2\Delta}\frac{\pi}{\eta_p}\left(\cot\frac{\pi}{\eta_p}+\sigma\right)\frac{1-\epsilon_s}{\mu_1-\mu_\Delta}\right]^{1/3}} \qquad -----(7)$$

That the actual problem falls into this case is indicated by the condition:

$$H_c \leq H_{nopt} \leq H_k \qquad -----(8)$$

With commonly encountered values of the parameters, the cubic root term in (7) is around unity. For Alnico V, H_k is about three quarters

of H_c . Therefore, the condition (8) is scarcely fulfilled.

STABILIZATION ON THE UPPER PART OF THE DEMAGNETIZATION CURVE: On this part of the demagnetization curve, equation (2) must be modified by substituting μ_u for μ_l and B_{ru} for B_{rl} . Also, for most common materials, μ_u is very close to μ_Δ . The condition for the actual problem to fall into this case is, instead of (8):

$$H_k \leq H_n \leq 0 \qquad \text{-----(9)}$$

The peak air gap flux density is given by, for any values of λ and m :

$$\hat{B}_g = \frac{(1-2\tau)\, B_u}{(1+\lambda)\left\{ A_{eo} \frac{\pi}{n_p} \left(\cot \frac{\pi}{n_p}\right) + \frac{2\Delta}{m} \right\}} \cdot \frac{1}{1+\frac{\mu_u}{1+\lambda} m} \qquad \text{-----(10)}$$

The optimum conditions are:

$$\lambda - \text{ as small as possible} \qquad \text{-----(11)}$$

$$m_{opt} = \sqrt{\frac{2\Delta}{A_{eo}} \frac{1+\lambda}{\mu_n \frac{\pi}{n_p} \cot \frac{\pi}{n_p}}} \qquad \text{-----(12)}$$

The other optimum quantities are:

$$\hat{B}_{g\,opt} = \frac{(1-2\tau)\, B_{ru}}{(1+\lambda)\left\{ \left(A_{eo} \frac{\pi}{n_p} \cot \frac{\pi}{n_p}\right)^{\frac{1}{2}} + \left(\frac{2\Delta}{m} \frac{\mu_u}{1+\lambda}\right)^{\frac{1}{2}} \right\}^2} \qquad \text{-----(13)}$$

$$H_{n\,opt} = \frac{-B_{ru}}{\mu_n \left\{ 1 + (\epsilon_s+\lambda) \left[\frac{A_{eo}}{2\Delta\mu_u} \frac{\pi}{n_p} \cot \frac{\pi}{n_p} \right]^{\frac{1}{2}} \right\}^2} \qquad \text{-----(14)}$$

In most commonly encountered case, the square root term in (14) is

around unity. While $\epsilon_s + \lambda$ has a small fractional value, the condition (9) is again scarcely fulfilled.

STABILIZATION AT THE KNEE: A glance on the expressions (7) and (14) reveals that the variable dominating the classification of the actual problem into the two cases is Δ . Because of the discontinuity at the knee, which is in reality a region of rapid change of slope, there is an interval of Δ which does not fall into either case. By far most useful cases fall into this category. Apparently, the optimum point of stabilization is then right on the knee.

As ϵ_s is given, the value of λ must be such that the point of stabilization is right on the knee, given by:

$$\lambda + \epsilon_s = - \frac{B_K}{H_K} m \qquad \text{-----(15)}$$

With this constraint taken into account, the following formulae hold:

For any values of m :

$$\hat{B}_g = \frac{(1-2\tau)(B_K - \mu_\Delta H_K)}{\left[A_{eo} \frac{\pi}{n_p} (\cot \frac{\pi}{n_p} + \sigma) + \frac{2\Delta}{m} \right] \left[1 - \epsilon + (\mu_\Delta - \frac{B_K}{H_K}) m \right]} \qquad \text{-----(16)}$$

The optimum conditions are

$$m_{opt} = \left\{ \frac{2\Delta}{A_{eo}} \cdot \frac{1-\epsilon}{\frac{\pi}{n_p} (\cot \frac{\pi}{n_p} + \sigma)(\mu_\Delta - \frac{B_K}{H_K})} \right\}^{\frac{1}{2}} \qquad \text{-----(17)}$$

$$\lambda_{opt} = - \left\{ \frac{B_K}{H_K} m_{opt} + \epsilon \right\} \qquad \text{-----(18)}$$

$$\omega = \frac{(1-2\tau)\pi}{\frac{2\Delta}{A_{eo} m} + \frac{\pi}{n_p} (\cot \frac{\pi}{n_p} + \sigma)} \cdot \qquad \text{-----(19)}$$

The optimum air gap flux density is:

$$\hat{B}_{g\,opt} = \frac{(1-2\tau)\,B_K}{\frac{\pi}{n_p}\left(\cot\frac{\pi}{n_p}+\sigma\right)\left\{\left[-2\Delta\,\frac{B_K}{H_K}\,\frac{1}{\frac{\pi}{n_p}\left(\cot\frac{\pi}{n_p}+\sigma\right)}\right]^{\frac{1}{2}}+\left[A_{eo}\,\frac{1-\epsilon}{1-\mu_\Delta\frac{H_K}{B_K}}\right]^{\frac{1}{2}}\right\}^2} \quad ----(20)$$

Typical values of air gap flux density are computed for a six pole machine and listed in Table I for illustrative purpose.

TABLE I

TYPICAL PEAK AIR GAP FLUX DENSITY
OBTAINABLE WITH OPTIMUM PROPORTIONS
(ALNICO V, 6-POLE ROTOR)

B_k - 9,500 gausses,	H_k - 475 oersteds,		- 4.0
B_{is}-19,000 gausses,	A_{do}' - 0.552,	A_{d1}'	- 0.942
- 0.04,	A_{eo} - 0.667,	A_{e1}	- 1.104

Δ	ν	$\hat{B}_g$
0.0025	0.15	8900 gausses
0.0025	1.0	7860
0.005	0.5	7620
0.005	1.0	6110

III THE OPTIMUM PROPORTION FOR MINIMUM WEIGHT OF THE MAGNETS WITH SPECIFIED AIR GAP FLUX DENSITY

THE CONSTRAINT IN THE PROBLEM: In many cases in practice, the maximum air gap flux density obtained with the optimum proportion given above may rise to too high an air gap flux density as to cause excessive saturation in the armature teeth. When this is the case, the entire available space in the pole sector needs not be utilized. Thus, the dimensional constraint is removed. The typical problem in this category is to find the optimum conditions for a minimum weight or volume of the magnet to yield a certain specified limiting value of the air gap flux density.

STABILIZATION ON THE LOWER PART OF THE DEMAGNETIZATION CURVE: For any values of λ and m :

$$\hat{B}_g = \frac{l_m}{\delta_e} \cdot \frac{m\,(\epsilon_s + \lambda + \mu_\Delta m)\, B_r l}{(\epsilon_s + \lambda + \mu_l m)\,(1 + \lambda + \mu_\Delta m)} \qquad \text{-----(21)}$$

The optimum conditions are:

$$\lambda_{opt} = \sqrt{\{(1-\epsilon_s)(\mu_l - \mu_\Delta)m\}} - \mu_\Delta m - \epsilon \qquad \text{-----(22)}$$

$$m_{opt} = \frac{1-\epsilon_s}{\mu_l - \mu_\Delta} \qquad \text{-----(23)}$$

The corresponding length of magnet is:

$$l_{m\,opt} = 4\,(\mu_l - \mu_\Delta)\,\frac{\hat{B}_g}{B_{rl}}\,\delta_e \qquad \text{-----(24)}$$

That the actual problem falls into this case is to be checked by (8) with value of $H_{n\,opt}$ given by:

$$H_{n\,opt} = -\frac{B_r l}{2\,(\mu_D' - \mu_\Delta)} \qquad \text{-----(25)}$$

Apparently very few commonly encountered materials can fulfill this condition.

STABILIZATION ON THE UPPER PART OF THE DEMAGNETIZATION CURVE: The optimum conditions are:

$$\lambda - \text{ as small as possible} \qquad \text{-----(26)}$$

$$m_{opt} = \frac{1+\lambda}{\mu_u} \qquad \text{-----(27)}$$

Other optimum quantities are:

$$l_{m\,opt} = 2\mu_u \frac{\hat{B}_g}{B_{ru}} \delta_e \qquad \text{-----(28)}$$

$$H_{n\,opt} = -\frac{B_{ru}}{\mu\left[1 + \frac{\epsilon_s + \lambda}{1 + \lambda}\right]} \qquad \text{-----(29)}$$

Again very few commonly encountered problems can meet the classification requirement given by (9).

STABILIZATION AT THE KNEE: Thus, it may be concluded that most commonly encountered problems fall into the case of stabilization at the knee. The optimum quantities are then given by:

$$m_{opt} = -\frac{H_K}{B_K}(\epsilon_s + \lambda) \qquad \text{-----(30)}$$

$$\lambda_{opt} = \frac{1 - 2\epsilon_s + \mu_\Delta \frac{H_K}{B_K}}{1 - \mu_\Delta \frac{H_K}{B_K}}. \qquad \text{-----(31)}$$

$$l_{m\,opt} = -2 \frac{\hat{B}_g}{H_K} \delta_e \qquad \text{-----(32)}$$

IV CONCLUSION AND DISCUSSION

The solution of the problem of economic design of the permanent magnet excited alternators has been hitherto guided by rather general theory associated with empirical rules only. The more substantial and definite formulae presented herewith have been used to check several existing designs. The results have shown that appreciable improvements are possible. As indicated in a previous section, air gap flux density as high as 8.9 kilogausses is feasible. On the other hand, most existing designs seem to be too long to be economical.

Under certain conditions, a problem of the second type may be given a better solution by a consideration of the first type. For example,

with a specified length of the air gap, the optimum $\hat{B}_g$ may be too high. Then the length of the air gap may be continuously diminished until the optimum air gap flux density falls within limit. By means of this procedure, a machine of minimum reactance may be obtained.

In the foregoing analyses, σ and ϵ_s have been considered independent of λ and m in obtaining the optimum conditions. In order to make a partial justification of this assumption, $\hat{B}_g$ has been computed for a specific design with different values of m by means of (3) and plotted as shown in Fig. 2. The small crosses are optimum points computed by formulae (17) and (20).

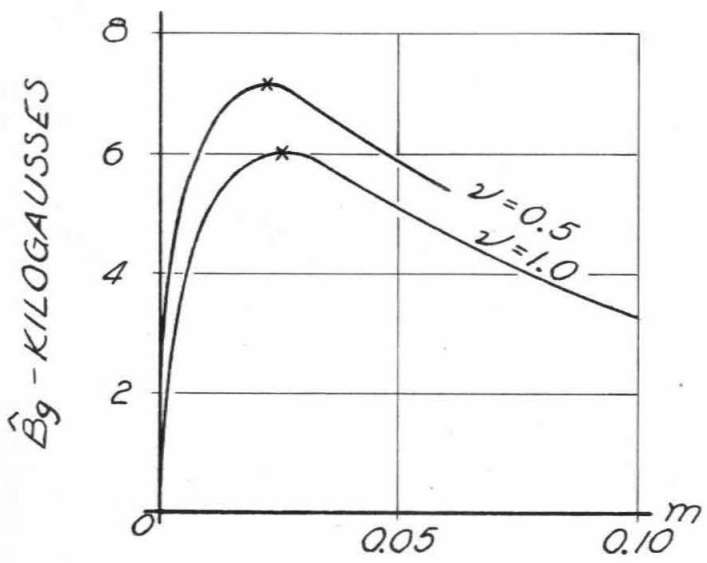

ALNICO V

ALL PARAMETERS SAME AS TABLE I

Fig. 2

APPENDIX I

THE DERIVATION OF THE FORMULA (1)

At the point of stabilization, with a pure inductive current, the reactance drop amounts to ν times the open circuit voltage, so:

$$I_s (x_{ld} + x_{ad}) = \nu K A_{e1} H_w l_m / \delta_e \qquad -----(33)$$

hence:

$$I_s = \frac{K \nu A_{e1} H_w l_m}{(x_{ld} + x_m A_{d1}) \delta_e} \qquad -----(34)$$

From the definition of ϵ_s , a relation is obtained between the flux and the potential at the pole piece:

$$\epsilon_s \frac{\pi A_{eo}}{n_p \Delta} (H_w l_m + \Pi \hat{F}_s) = (A_{eo} H_w l_m - A_{do} \hat{F}_s) \frac{\pi}{n_p \Delta} \qquad -----(35)$$

By the definition of the armature reaction reactance:

$$I_s x_{ad} = K A_{d1} \hat{F}_s / \delta_e \qquad -----(36)$$

hence:

$$\hat{F}_s = \frac{\nu A_{e1} I_s}{A_{d1} + x_{ld}/x_m} \qquad -----(37)$$

Eliminating I_s and $\hat{F}_s$ by combining (34), (35), and (37):

$$\epsilon_s = \frac{1 - \frac{A_{do}}{A_{eo}} \frac{\nu A_{e1}}{A_{d1} + x_{ld}/x_m}}{1 + \Pi \frac{\nu A_{e1}}{A_{d1} + x_{ld}/x_m}} \qquad -----(38)$$

If the armature slots are not skewed, the following relations hold:

$$\Pi = \Pi \approx \frac{A'_{do}}{(1+\lambda+\mu_\Delta m)A_{eo}} \qquad -----(39)$$

$$A_{do} = A'_{do} - \Pi_o A_{eo} \qquad -----(40)$$

Combining (39) and (40) into (38) leads to (1).

APPENDIX II

THE DERIVATION OF FORMULAE (3) AND (19)

As shown in Fig. 3, along the linear representation of the major loop:

$$B = B_{rL} + \mu_L H \qquad -----(41)$$

Along the external permeance line for the point of stabilization, i.e., OB_n :

$$B = -(\epsilon_s + \lambda)\, H/m \qquad -----(42)$$

Thus:

$$B_n = \frac{(\epsilon+\lambda)\, B_{rL}}{\epsilon_s + \lambda + \mu_{rL} m} \qquad -----(43)$$

$$H_n = -\frac{m\, B_{rL}}{\epsilon_s + \lambda + \mu_{rL} m} \qquad -----(44)$$

Along the linear representation of the minor loop:

$$B = B_n - \mu_\Delta H_n + \mu_\Delta H \qquad -----(45)$$

Along the external permeance line for open circuit, i.e., along OB_w :

$$B = -(1+\lambda)\, H/m \qquad -----(46)$$

Thus:

$$B_w = \frac{(1+\lambda)(\epsilon_s+\lambda+\mu_\Delta m)\, B_{rL}}{(\epsilon_s+\lambda+\mu_L m)(1+\lambda+\mu_\Delta m)} \qquad -----(47)$$

$$H_w = \frac{-m(\epsilon_s+\lambda+\mu_\Delta m)\, B_{rL}}{(\epsilon_s+\lambda+\mu_L m)(1+\lambda+\mu_\Delta m)} \qquad -----(48)$$

The open circuit peak air gap flux density is:

$$\hat{B}_g = -\frac{H_w l_w}{\delta_e} = \frac{l_m}{\delta_e} \frac{m(\epsilon_s+\lambda+\mu_\Delta m)}{(\epsilon_s+\lambda+\mu_L m)(1+\lambda+\mu_\Delta m)} \qquad -----(49)$$

The dimensional relations are shown in Fig. 4. The length y is determined by the condition that the pole tip must be capable to carry the maximum protective leakage flux without excessive saturation; thus:

$$\sigma = \frac{2y}{w} = \frac{\lambda}{\epsilon_s+\lambda} \frac{B_n}{B_{si}} \qquad \text{or} \qquad \frac{2y}{D} = \sigma\omega \qquad -----(50)$$

since $$l_m = \frac{D}{2}\left\{(1-2\tau)\pi - \frac{\pi}{n_p}\left(\cot\frac{\pi}{n_p}+\sigma\right)\omega\right\} \qquad -----(51)$$

we obtain:

$$m = \frac{\omega D}{l_m} \frac{\Delta}{A_{eo}\pi} = \frac{2\omega\Delta/A_{eo}}{(1-2\tau)\pi - \frac{\pi}{n_p}\left(\cot\frac{\pi}{n_p}+\sigma\right)\omega} \qquad -----(52)$$

so that:

$$\omega = \frac{(1-2\tau)\pi}{\frac{2\Delta}{m A_{eo}} + \frac{\pi}{n_p}\left(\cot\frac{\pi}{n_p}+\sigma\right)} \qquad -----(53)$$

which is the same as (19).

Substituting (51) into (49) leads to (3).

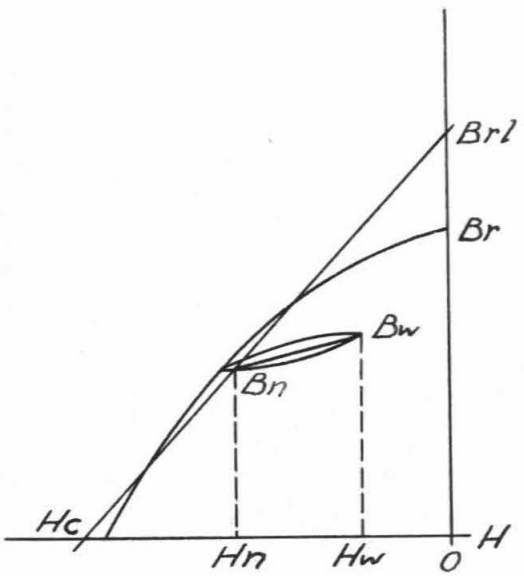

Fig. 3

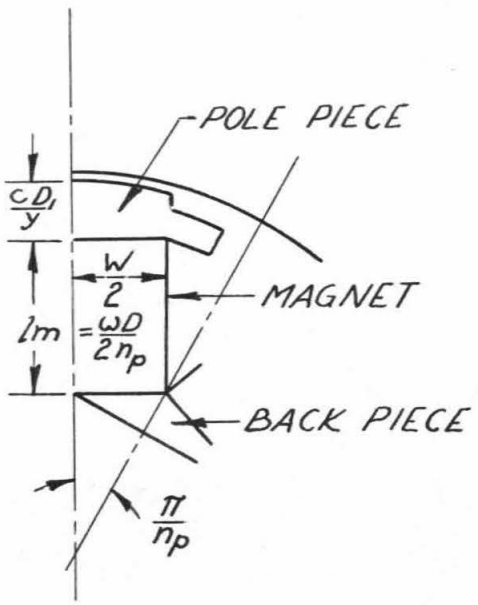

Fig. 4

APPENDIX III

THE DERIVATION OF OTHER FORMULAE

(4) Putting $\frac{\partial \hat{B}_g}{\partial \lambda}$ from (3) to zero.

(5) Substituting (4) into (3) and putting $\frac{d \hat{B}_g}{d \sqrt{m}}$ to zero.

(7) Substituting (4) and (5) into (44).

(10) Substituting μ_u for both μ_1 and μ_Δ in (3).

(11) $\frac{\partial \hat{B}_g}{\partial \lambda}$ is always positive.

(12) Putting $\frac{\partial \hat{B}_g}{\partial m}$ from (10) to zero.

(13) Substituting (12) into (10).

(14) Substituting (12) into (44).

(16) Substituting (15) into (3).

(17) Putting $\frac{\partial \hat{B}_g}{\partial m}$ from (16) to zero.

(18) Substituting (17) into (15).

(20) Substituting (17) into (16).

(22) Same as (4), putting $\frac{\partial \hat{B}_g}{\partial \lambda}$ from (21) to zero.

(23) Substituting (22) into (21), solving for l_m. The volume of the magnet is then given by $m p_g l_m^2$. Put the partial with respect to m to zero.

(24) Substituting (22) and (23) into (21).

(25) Substituting (22) and (23) into (44).

(27) Substituting μ_u for both μ_1 and μ_a into (21). Rest being the same as (23).

(28) Substituting μ_u for both μ_a, μ_1 in (21) and combine with (27).

(29) Substituting (26) and (27) into (44).

(31) Substituting (30) into (21), so expressing the volume of the magnet in terms of λ. Differentiating with respect to λ. Putting the derivative to zero.

(32) Substituting (31) into (21).

APPENDIX IV

SYMBOLS AND DEFINITIONS

A_{do} Ratio of the average value of the air gap flux density to the peak value, under the action of the direct axis armature reaction.[6]

A'_{do} The same with zero magnet reluctance.[6]

A_{d1} Ratio of the maximum of the space fundamental of the air gap flux density to the peak value, under the action of the direct axis armature reaction.[6]

A_{d1}' The same with zero magnet reluctance.[6]

A_{eo} Same as A'_{do} but under the action of the excitation alone.[6]

A_{e1} Same as A_{d1} but under the action of the excitation alone.[6]

$\hat{B}_g$ The peak value of the air gap flux density for open circuit.

B_k The magnetic induction in the magnet at the knee of the demagnetization curve.

B_n The magnetic induction in the magnet at the point of stabilization.

B_r The remnant magnetic induction of the magnetic material.

B_{rl} The B-intercept of the linear representation for the lower part of the demagnetization curve.

B_{ru} The same for the upper part of the demagnetization curve.

B_{si} The maximum permissible magnetic induction in the pole tip.

B_w The magnetic induction in the magnet at the point of open circuit.

D The diameter of the rotor.

$\hat{F}_s$ The maximum of the space fundamental of the direct axis armature reaction mmf.

H_c The coercive field intensity of the magnet.

H_k The field intensity in the magnet corresponding to the knee.

H_n The field intensity in the magnet corresponding to the point of stabilization.

H_w The field intensity in the magnet corresponding to open circuit.

I_s The demagnetizing armature current against which the magnet is to be stabilized.

K The winding constant, defined as the ratio of the induced voltage to the maximum of the flux density.

l_m The length of the magnet.

m $\frac{p_m}{p_g} \frac{w}{\pi l_m} \frac{n_p \Delta}{A_{eo}}$

n_p Number of poles.

p_e Permeance external to the rotor (equivalent value), at the point of stabilization, ratio of the total flux emerging from the pole face to the potential of the pole piece.

p_g The air gap permeance.

p_l The internal leakage permeance.

p_m The permeance of the magnet, assuming unit permeability.

w The width of the magnet.

χ_{ad} The direct axis armature reaction reactance.[6]

χ_{al} The direct axis leakage reactance.[6]

y The part of the thickness of the pole piece allowed for the protective leakage flux.

Δ The ratio δ_e/D .

δ_e The effective length of the air gap.

ϵ_s The ratio ϕ_e/ϕ_g .

λ The ratio ϕ_l/ϕ_g .

σ The ratio $\frac{\lambda}{\epsilon_s+\lambda}\frac{B_r}{B_{si}}$.

μ_l The slope of the linear representation of the lower part of the demagnetization curve.

μ_u The same for the upper part.

μ_Δ The same for the minor loop.

ω The ratio $n_p w/D$.

τ The ratio of the minimum thickness of the pole piece to the diameter.

ν Voltage stability factor.

Π Ratio of the scalar magnetic potential of the pole piece to the maximum of the space fundamental of the armature demagnetizing mmf producing the potential.

Π_o The same with parallel armature slots.[6]

REFERENCES

1. Hornfeck and Edgar - The Output and Optimum Design of Permanent Magnets Subject to Demagnetizing Force - A.I.E.E. Trans.Vol.59, pp. 1017-24.

2. Desmond - The Economic Utilization of Modern Permanent Magnet Materials - Journal of I.E.E. (London), Vol. 92, pp. 229-52.

3. Sanford - Permanent Magnets - U. S. National Bureau of Standards Circular C448 (August 10, 1944).

4. Underhill - Designing Stabilized Permanent Magnets - Electronics Vol. 17, p. 118.

5. Cioffi - Stabilized Permanent Magnets - A.I.E.E. Trans.Vol. 67, pp. 1540-43.

6. Luo - The Synchronous Reactances of Alternators with Permanent Magnet Excitation and Alternators with Skewed Slots.